TAMPEREEN TEKNILLINEN YLIOPISTO
TAMPERE UNIVERSITY OF TECHNOLOGY

ABDUL MANNAN

IMPROVING HYDRAULIC BOOM CONTROL BY IMPROVED TRAJECTORY PLANNING AND IMU BASED JOINT ANGLE FILTERING

Master of Science Thesis

Examiner: prof. Reza Ghabcheloo
Examiner and topic approved on 28th February 2018

ABSTRACT

Abdul Mannan: Improving hydraulic boom control by improved trajectory planning and IMU based joint angle filtering
Tampere University of technology
Master of Science Thesis, 56 pages
March 2018
Master's Degree Programme in Automation Engineering
Major: Factory Automation and Industrial Informatics
Minor: Industrial Management
Examiner: Professor Reza Ghabcheloo

Keywords: IMUs (Inertial measurement units), Trajectory Planning, IMU filtering, Real-time Simulink, XPC target

This research is carried out under the project of Autonomous Earth moving. In this project Generic Intelligent Machine (GIM) is used to dig up the pile and afterwards dumping it to a user defined position autonomously. However, there are few problems reported in the initial iteration of the project. This thesis focuses on solving these issues. One of the problem is the unnecessary oscillation of the boom and the bucket of GIM machine while moving from the one position to another. Second problem is related to the boom positioning in the steady state. As the boom and the bucket are interlinked, therefore mispositioning of boom induces an error in the positioning of the bucket, which causes major issue during the scooping phase.

For removing unnecessary oscillation trajectory planning has been introduced for moving the manipulator from current position to the desired positions. In this approach, interim intermediate positions are introduced between the current and a desired position, which the hydraulic manipulator follows. This technique also divides the whole value of the error between the user defined positions. While for the problem of the boom positioning in the steady state, IMU filtering performance is improved. The approach proposed is to remove the linear accelerations from the data of the accelerometer prior to the complementary filter. Afterwards, the complementary filter produces the accurate steady state boom angle for the positioning of the boom.

The results after implementing these approaches show that the individual problems are being solved. Trajectory planning has removed most of the unnecessary oscillations. However, still there are few oscillations remaining where the manipulator is moved from haul to dump. Second approach of IMU filtering has greatly improved the results as now complementary filter is capable of reducing overshoots in the boom angle during steady state. However, few overshoots can still be seen in the overall response.

PREFACE

I will start by thanking my supervisor Prof. Reza Ghabcheloo for his continuous motivation and support in every step of my thesis. He has always been supportive and guided me whenever I had any trouble. I would also like to thank Eric Halbach, Antti Kolu, and Mika Hyvonen, who helped me a lot during the course of my thesis especially during the Testing Phase.

I would like to thank my family for their love and support as without them I would never have been able to complete my studies. I would especially like to thank my friend Shadman Razzaq Siddiqui, who guided me with his experience. Last but not the least I would like to thank Ihtisham Ali, Muhammad Usman, Shahbaz Ali and Umer Iftikhar who supported during the course of my studies.

Tampere, 24.4.2018

Abdul Mannan

TABLE OF CONTENT

LIST OF FIGURES

LIST OF TABLES

LIST OF SYMBOLS AND ABBREVIATIONS

AFS	Articulated frame steering
AUT	Laboratory of Automation and Hydraulics
FIR	Finite Impulse response
GIM	Generic Intelligent Machine
GNSS	Global Navigation Satellite system
HIL	Hardware in loop
IIR	Infinite Impulse Response
IMU	Inertial Measurement Unit
MEMS	Micro-electromechanical systems
RMS	Root mean square
b	Bias
m	Mass
x	Mass displacement
$\dot{x}$	Velocity of the mass
$\ddot{x}$	Acceleration of the mass
ε	Noise
$\dot{\theta}$	angular velocity
ω_g	angular velocity from gyroscope
a_x	acceleration component in x-axis
a_z	acceleration component in z-axis
θ_a	angle calculated from the data of accelerometer
x	Position of FF in x-axis
z	Position of FF in z-axis
θ	Orientation of bucket
FF_f	Desired position of FF point
FF_i	Initial position of FF point
x_i	x-coordinate of IMU frame
z_i	z-coordinate of IMU frame
x_b	x-coordinate of boom frame
y_b	Z-coordinate of boom frame
V_x	Velocity of link in x-axis
V_z	Velocity of link in z-axis
${}^bV$	Velocity of boom
${}^bR_i$	Rotation matrix of IMU with respect to boom
L	Length of the link
$\ddot{\theta}$	Angular acceleration
a_{lx}	Linear acceleration of boom in x-direction
a_{lz}	Linear acceleration of boom in z-direction

1. INTRODUCTION

1.1 Overview

In recent years, there have been many joint ventures between automotive industry and software companies for introducing Autonomous vehicles technology in the near future [1]. To compete in this race, Department of Automation and Hydraulics (AUT) has initiated many projects for autonomous mobile machines. One of the projects is the autonomous earth moving. In this project, a Generic Intelligent Machine (GIM) with a boom and a bucket, is used to dig up the pile and dump it at the user-defined positions using high-level plan. A few problems have been reported during the implementation of this process. A core issue is the unnecessary oscillations of the boom and the bucket while actuating from one position to another. Furthermore, boom angle from complementary filter is not accurate during the steady state, as the linear acceleration from accelerometer are not being removed, which effects the positioning of boom. Boom and bucket are interlinked, therefore mispositioning of boom affects the position of the bucket of the GIM machine. Therefore, often bucket does not position parallel to the ground during digging i.e. it is either pitched upwards or downwards. These errors in the motion state sense are due to the errors of the Inertial Measurement Units (IMUs). In this study, an attempt is made to minimize these errors with two different approaches. One of the approaches is to introduce the trajectory planning for the movement of the GIM machine's boom and bucket from one position to another. With the help of trajectory planning, interim intermediate states are introduced between the current and a final position. As a result, the error is distributed over the range into smaller portions. Thus, the boom and the bucket can have a smoother movement. The second approach is to improve the performance of IMU with filtering. The IMU utilized is composed of two MEMS sensors i.e. two-axis accelerometer and one-axis gyroscope [2]. Complementary filter uses the data of gyroscope and accelerometer to calculate the boom angle. Complementary filter calculates boom angle in the transient state through the gyroscope while the accelerometer is used to determine the boom angle in the steady state. Unfortunately, the boom angle calculated from the accelerometer is not accurate because of the linear accelerations in the data of the accelerometer. Therefore, to calculate the angle correctly from an accelerometer, linear accelerations are to be removed prior for the complementary filter.

The thesis is organized in the following manner. Chapter 2 introduces the theoretical background to understand the underlying concepts. Chapter 3 represents the current system and the methodology adopted to improve the current system with the help of two proposed approaches in order to achieve the desired results. Chapter 4 explains the first approach in detail that is the Trajectory Planning with its testing results. Chapter 5

describes the second approach in detail that is the improvement of the IMU filtering. Finally, chapter 6 concludes the thesis followed by the future aspects in this field.

1.2 Autonomous Earth Moving Project

In the recent years a lot of research has been carried out to perform different tasks using autonomous vehicles or autonomous mobile machines. These research projects have changed according to the time and the need of the market. Laboratory of Automation and Hydraulics (AUT) at Tampere University of Technology (TUT) works with similar kind of projects, one of which is the Autonomous Earth Moving. The main task of this project is to use a robotic wheel loader for pile transferring. The mobile machine used for this purpose is an AVANT 635-wheel loader machine, which is modified for research purposes and will be referred as the Generic Intelligent Machine (GIM) here after. In this project, a ground model is created with the use of on-board laser scanner. The system scans the environment and classifies the areas of digging and dumping, afterwards storing it in the High-level plan. Using the high-level plan, GIM autonomously digs up the pile and dumps it at the user defined position. Meanwhile the ground model is updated iteratively based on the remaining pile. There are three states in which this task is completed. First is the scoop state in which the machine digs up the pile, second is the haul state in which the machine carries the pile towards the dumping point. Third is the dump state in which the machine dumps the pile. In the implementation of earth moving operations, few problems arise which will be explained in the following section.

1.3 Problem Statement

In the initial iterations of the Autonomous earth moving project's implementation, there are few issues that are reported. One of which is the unnecessary oscillation of the boom and the bucket during the transition from one state to another. The subsequent issue is regarding the miscalculation of boom angle in the steady state, as boom and bucket are interlinked it leads to the misalignment of the bucket while scooping i.e. if the bucket's cutting blade is not parallel to the ground and is either upwards or downwards it will not scoop the pile effectively and may drive up the pile or scratch the ground during the process. Which results in the failure of the system.

1.4 Proposed solution

In order to minimize the oscillations between the two states of the process and accurate positioning of the bucket for scooping, this study proposes two approaches to solve this problem. First approach is to introduce the trajectory planning for smooth transition between the states. The controller actuates the boom and the bucket from one state to the

next by minimizing the error between the current and the desired point. Using trajectory planning with first order polynomial, intermediate positions are created within the different states, causing the error to be divided within these positions. The end result is a smooth transition from one state to the next. The second approach is regarding the IMU filtering. The system calculates the boom angle through complementary filter by using the data of the gyroscope and the accelerometers. The major issue with the current system is that the boom angle is not accurate in steady state, because linear accelerations are not being filtered out prior to the complementary filter. Therefore, a technique is proposed to calculate the linear acceleration of the boom and to remove it from the data of accelerometer prior to complementary filter. Thich will enable the system to calculate accurate boom angle during the transient state as well as in the steady state.

1.5 GIM machine

Laboratory of automation and hydraulics (AUT) of Tampere University of Technology (TUT) and System Technology of Aalto university collaborated for the research project named as GIM. The aim behind this research is to develop technologies for future autonomous mobile work machines [1].

GIM machine is the Articulated-frame steering (AFS) machine with the model name as AVANT 635. GIM machine consist of two separate parts front part and the back part which are connected with the single articulated joint or a hinge [1]. At present, the front auxiliary part attached to the GIM machine is the Boom which has an articulated joint for the moment and the telescopic joint for its extension. There are also many sensors attached to the GIM machine like Inertial Measurement Unit (IMUs), Hall sensors, laser Scanner, and Global Navigation Satellite system (GNSS) sensors. GIM machine is also equipped with the XPC target and the Linux pc for running and controlling different sensors and actuators.

As mentioned earlier, in this thesis the focus will be on the movement of the boom and the bucket of the GIM machine. There are three IMUs attached to the GIM machine; one on the base, then on the Boom for measuring its position and last one is on the bucket for its position measurement.

Figure 1: GIM Machine

2. THEORETICAL BACKGROUND

2.1 IMUs (Inertial measurement Units)

IMU is a compact package of gyroscope and accelerometer, used to estimate relative position, angular motion, and linear motion of the system in every direction. In other words, IMU estimates the position (in three-dimensional axis) and also the orientation (roll, pitch, and yaw) of a system. This estimation is only possible with the help of three orthogonal gyroscopes and three orthogonal accelerometers. Gyroscope provides the angular velocity (ω). While the accelerometer is used to determine the instantaneous acceleration of the system. [2]

2.1.1 Gyroscope

Gyroscope is a device that can be used to measure angular velocity either relative to certain inertial frame of reference or with the angle turned through by a vehicle or structure. Gyroscope working principle is the law of conservation of angular momentum, which is one of the Newtonian law [3]. Angular momentum is the property of rotating object to keep the object rotating until some external force hinders its motion. this feature allows them to use in different type of roles like [4]:

- Navigation
- Stabilization
- Autopilot feedback

There are three types of gyroscopes:

1. Mechanical gyroscope (Rate gyros)
2. Optical gyroscope
3. MEMS

Mechanical gyroscope

This type of gyroscope works on the principle of inertial properties, in which is rotor or wheel spinning at high speed. Systems with constant angular momentum retain their angular momentum and direction until or unless they are isolated by external torque. This property of rigidity of the spin axis give rise to another property and that is how the system will respond to external torques, this property is known as precession [3]. In other words, when external torque is applied to the object for altering the axis of rotation, this changes the direction of the spin due to the law of conservation of angular momentum. This change is perpendicular to the direction of angular momentum and the direction of applied torque. Furthermore, this change is measured in order to measure angular velocity.

Mechanical Gyroscope is illustrated in the figure below in which rotor is fixed in a set of frames or gimbals in which it can able to rotate freely with respect to one another. [4]

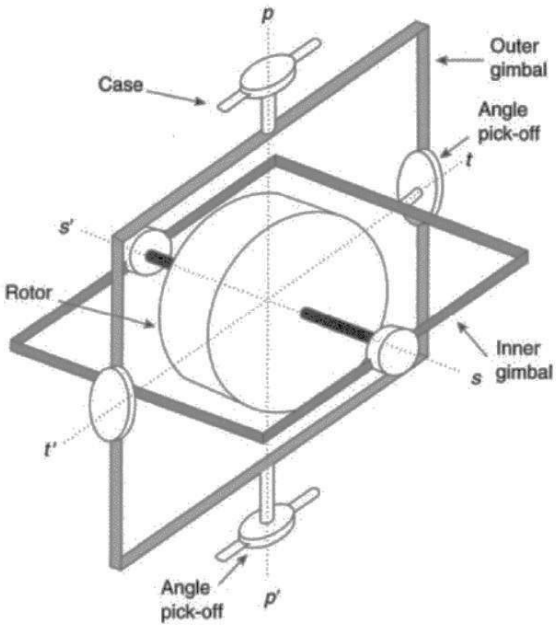

Figure 2: Two axis mechanical gyroscope [4]

These gyroscopes have complex working principal which increases the cost, size and delicacy of the instrument. That's why advance research in this technology give way to the less expensive and more reliable instruments that are optical gyroscopes [3].

Optical Gyroscope

An optical gyroscope uses the Sagnac effect to measure the angular rotation, which is the versatile technique for this type of measurement. Unlike the mechanical gyroscope, this type of gyroscope does not have moving parts and cannot be affected by shocks or vibrations. This is the main reason why optical gyroscopes have low maintenance. This feature of optical gyroscopes has made them suitable in the field of radar, robotics, aeronautics, automotive and gaming. [5]

Optical gyroscope has two types, namely:

- Ring laser gyroscope
- Fiber optic gyroscope

They both works on the principle of Sagnac effect rather than using the principle of rotational inertia like in mechanical gyroscope. For sagnac effects, two beams of light are made to follow the same path in ring but both beams are travelling in opposite direction; after exiting the ring both beams undergo the interference and the phase difference between these beams is measured. According to this principle, phase difference between

the beams is proportional to angular velocity. Optical gyroscopes are quite more accurate because of two counter-rotating beams of light are introduced in the system and these beams are sensitive to the device's axis of rotation, as beam cover more distance in the rotating direction than the direction. When these counter rotating beams are combined; interference occurs between them which is measurable to find the signal proportional to angular velocity. [6]

This principle is demonstrated in the figure below

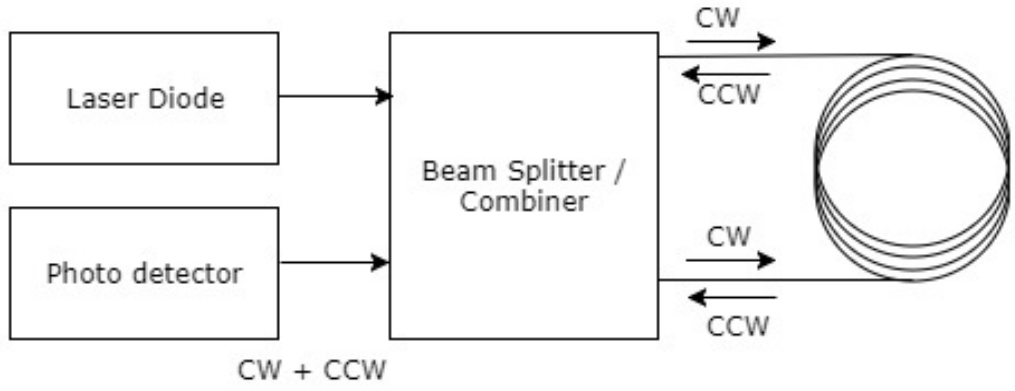

Figure 3: Fiber Optic Gyroscope

Accuracy of Ring laser gyroscope is more than the Fiber optic gyroscopes. Ring laser gyroscope uses the lasing medium for travelling of beams and ring itself is also a laser. When two beams are combined, they produce the beat frequency which is proportional to angular velocity. However, this makes the ring laser gyroscope quite expensive. On the other hand, Fiber optic are cheaper and simple to use. In fiber optic gyroscopes, laser diode produces the signal which is sent in opposite direction around the fiber optic coil. After exiting the coil, both signals are combined, and phase difference is being measured using photodetector. The measured phase difference is proportional to the angular velocity. [6]

MEMS Gyroscope

MEMS (micro-electromechanical system) gyroscopes are quickly replacing mechanical and optical gyroscopes because they have no rotating parts, extremely small and have low power consumptions [3]. MEMS (micro-electromechanical system) gyroscope measures the rotation based on vibrating mechanical elements. These vibrating mechanical elements produces the Coriolis force as the transfer of energy is occurring between the vibratory modes. Coriolis force is an inertial force which acts on the object moving relative to reference rotating frame [7]. In MEMS gyroscope, velocity is induced in the proof mass due to Coriolis force, in one direction and then angular velocity is measured in orthogonal axis because of the device rotation. In other words, Coriolis coupling is

behind the whole operation of gyroscope, because it enables the transfer of drive energy to the sense mode because of the angular velocity. This transfer of energy make the proof mass flexures to vibrate along perpendicular directions to achieve the Coriolis coupling [6]. This idea is shown in the figure below:

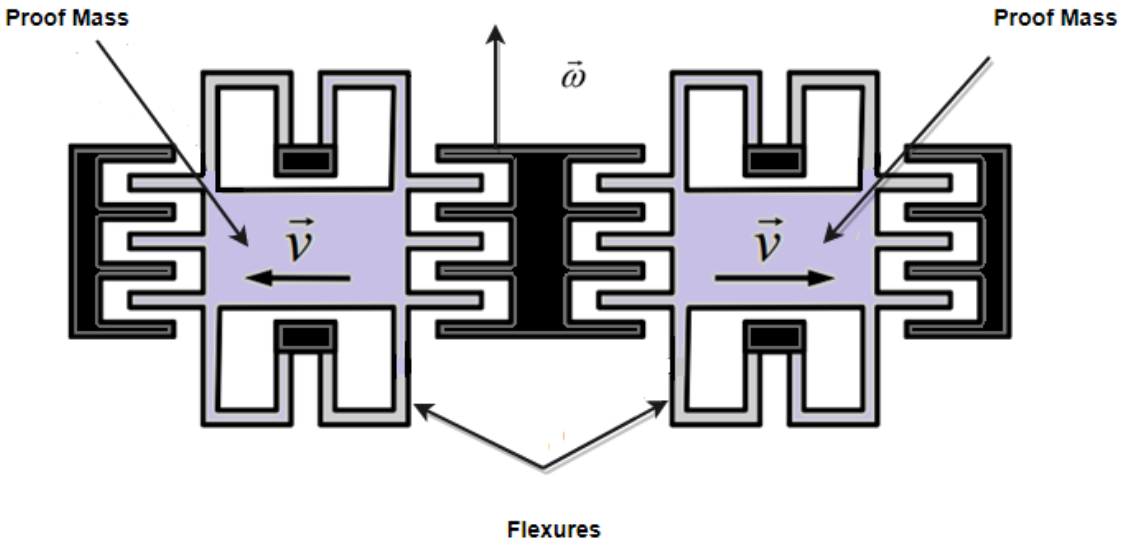

Figure 4: Internal assembly of MEMS gyroscope [6]

Figure 3 illustrates the model of the internal assembly of the MEMS gyroscope, comb fingers are working as small electrostatic motors inducing required oscillations. Darker areas are fixed boundaries of the model. While lighter areas are the proof mass which oscillates left and right out of phase according to the induced Coriolis force because of the rotation around vertical axis of the page. The capacitor plates above and below the proof masses are used to sense the out of plane motion.

Coriolis acceleration can be expressed in the form of equation which is as follows [3]:

$$a_{cor} = 2v \times \Omega \tag{1}$$

In equation 1, a_{cor} is the Coriolis acceleration. Whereas v is the local velocity of the object moving in straight line in a rotating frame whereas at Ω is the rate according to an inertial frame.

Errors

There are certain limitations of Gyroscope which effects the performance of a gyroscope. Some of those errors are listed below [3]:

1. Bias Repeatability:

   Bias is the drift of the gyroscope.

2. Angle random walk:

   This is the external or electronic noise in the data from gyroscope.

Scaling factor is also very important while taking the readings from gyroscope because there is some intrinsic sensitivity in mechanical system of gyroscope. Secondly there are also some deflections or mechanical stress produced by Coriolis force. Therefore, output scale factor is highly needed for reading, which can easily be get through electronic gain [4]. So, the equation for gyroscope is as follows.

$$\omega_g = K\dot{\theta} + b + \varepsilon \tag{2}$$

In equation 2, Gyroscope sends ω_g, which contains angular velocity, bias, and noise. Whereas, $\dot{\theta}$ is angular velocity of the sensor and K being the scaling factor (for correct estimation of gyroscope readings), b is the drift of gyroscope known as bias and ε is the noise of the gyroscope.

2.1.2 Accelerometer

Accelerometer measures the external forces on the vehicle. They are used to measure all the external forces including force of gravity. Basically, Accelerometers convert accelerations into deflections or stress deviation [8].There are three types of accelerometer that are as follows [3]:

1. Mechanical accelerometer
2. Piezoelectric accelerometer
3. MEMS accelerometer

Mechanical accelerometer

These accelerometers are based on the principle of measuring the relative displacement of small mass attached to the case by a spring. This mechanism is called mass-damper-spring system as illustrated in the figure 4. The force applied on the system and the distance displaced by the mass can be expressed with the help of the following equation [3].

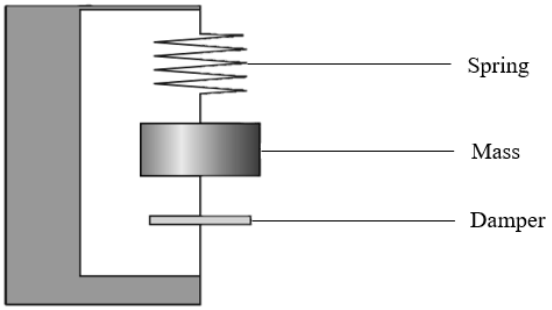

Figure 5: Mass-damper-spring system

$$F_{applied} = F_{due\ to\ mass} + F_{damping} + F_{spring}$$

$$= m\ddot{x} + c\dot{x} + kx \quad (3)$$

Where,

$$m = mass\ of\ the\ body$$

$$c = damping\ constant$$

$$x = mass\ displacement$$

$$\dot{x} = velocity\ of\ the\ mass$$

$$\ddot{x} = acceleration\ of\ the\ mass$$

There are certain limitations of the mechanical accelerometers that they are very sensitive to the mechanical vibrations or shocks.

Piezoelectric Accelerometer

This accelerometer doesn't contain any measurement of mechanical forces. It consists of piezoelectric crystal, mass, and spring. Mass is suspended over the crystal if any force acts upon the mass, it is directly related to the crystal, which induces the voltage depending upon the magnitude of the force [3]. This principle is explained in the figure 6:

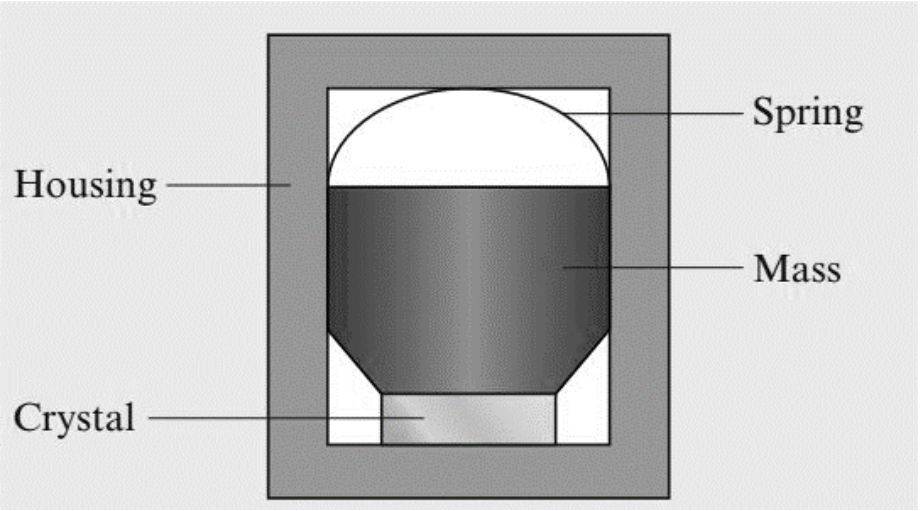

Figure 6: Piezo-electric accelerometer [3]

These accelerometers have some drawbacks as we can see in the figure 5 that piezoelectric element has mechanical contact with the base, so it makes it sensitive to the base bending and thermal transients. Thus, errors in the signal might have those impacts which can be large. [9]

MEMS Accelerometer

MEMS technology has advanced in the last decade rapidly. In this research semi-conductor design and fabrication principle is introduced in the mechanical systems that can vibrate due to the external forces in order to sense motion. There are several design categories for MEMS accelerometer, one showed in the figure 3 is the in-plane mass displacement design. [6]

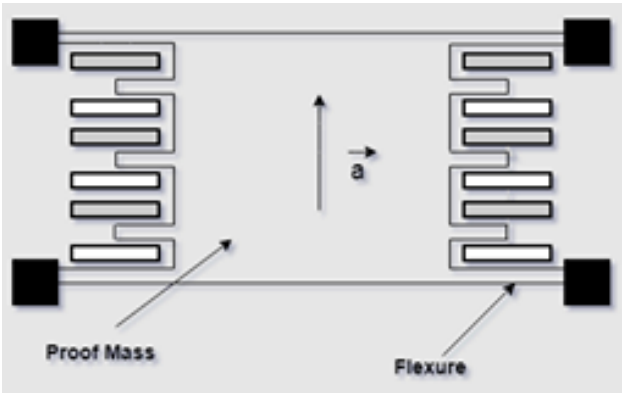

Figure 7: In-plane mass displacement design

In this case, proof mass is placed in the flexures and it can be deflected under acceleration which results in the change of gaps between the comb fingers, ultimately changing the overall capacitance between all pairs of fingers. External acceleration allows the proof

mass to oscillate in the plane of wafer. This external acceleration can be measured by the change in the resonant frequency of the device. [6]

Recent development in the MEMs technology provides us the opportunity of using three accelerometers in a single chip, which enable us to get the acceleration in every direction of the coordinate system i.e. x, y, and z.

Some external force acting on an object can be measured through accelerometer because it gives the component due to gravity and linear acceleration due to movement of the object in their respective axes. Keeping in mind these accelerations are in the sensor frame. This can be represented as follows:

$$a_x = g \sin\theta + a_{lx} \tag{4}$$

$$a_y = g \cos\theta + a_{ly} \tag{5}$$

Where $a_x$is the value from accelerometer in x-axis, a_y is the value from accelerometer in y-axis, and a_l is the linear acceleration in their respective axes. While θ is the angle of sensor respect to gravity and g is the acceleration because of gravity.

This data from accelerometer can easily be manipulated to get the required angles. This can be done by dividing equation (5) by equation (4) and then applying inverse tan to it. [arctan [a_y / a_x]].

So, result we get is as follows:

$$\theta_{acc} = \theta + \varepsilon_2 \tag{6}$$

2.2 Filters

The word filter in electronics is inspired and adopted from its generic meaning. A filter is anything that is capable of separating unwanted part from the core system. In the era of radios, electronic filters were introduced. These filters are of physical nature and used to attenuate the unwanted frequencies. Later, this concept was expanded to the separation of the noise from the signal. These filters were called the passive filters. In the current era of digitalization, most filters are designed inside the software. These digital filters are immensely useful for processing of the data.

Adaptive Filter

Adaptive filters are the dynamical system with variable or adaptive parameters. Adaptive filter modifies the value of its parameters through their transfer function. In these filters input signal is processed with the transfer functions in order to mitigate the noise or interference signals. The operation of the adaptive filter is the estimation of the statistical properties of the signal while changing the parameters to achieve the desired results. The core property in adaptive filtering is the estimation of parameter [coefficient of the transfer function] of the filter. [10]

There are several types of filters that come under the section of adaptive filters such as Finite Impulse Response (FIR) filter, infinite Impulse Response (IIR) filter and Complementary filter. Considering the scope of this study, we will restrict our discussion to complementary filters.

Complementary Filter

Complementary filter was introduced in 2007 by Shane Colton [11,12]. A complementary filter deal with the signals which are in frequency domain only. Complementary filter analyses the signal in their frequency domain later signals are combined for the better estimation of a particular quantity [13]. Complementary filter can be used directly without any pre-calculations, since, no assumptions are needed for linearity or noise statistics [14]. Complementary filter is widely used for attitude estimation from the IMUs (Inertial Measurement Units) readings. Complementary filter is composed of high pass and low pass filter. For the attitude estimation in IMUs, high pass filtering is performed on angular velocities provided by the gyroscope while performing low pass filtering on the accelerometer data, to eliminate high-frequency noise [13]. Thus, the combination of the two-filtered data provides the accurate and noise free estimation of attitude [15].

Complementary filter uses accelerometer and gyroscope simultaneously for estimating the best possible results of attitude. Initially, complementary filter relies on the data from gyroscope, since the data is precise and not susceptible to external noises. However, in the long run complementary filter shifts to the data of the accelerometer in order to avoid the drift because of the gyroscope [11]. This principle is shown in the following diagram:

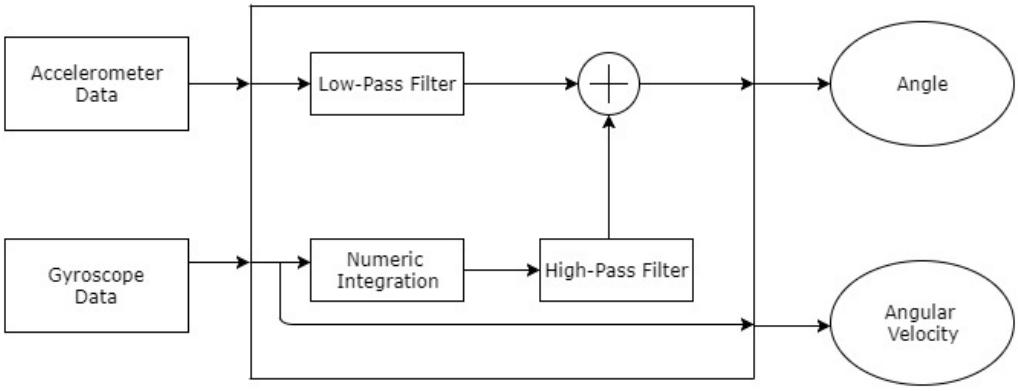

Figure 8: Complementary filter algorithm

In Figure 8, function of the low pass filter is performed on the data of accelerometer, to filter out the short-term response from it, because accelerometer has accurate response in the long term. The high pass filter performs the same task for the data of gyroscope for filtering out the long-term response of the gyroscope, because it has accurate response in the short-term [11]. Mathematical representation of this filter in comparison to our system is as follows:

$$\theta_{boom} = \alpha * (\theta_{boom} + \dot{\theta} * dt) + (1 - \alpha) * \theta_a \tag{7}$$

Whereas

$$\theta_{boom} = Boom\ angle$$

$$\alpha = filter\ coefficient$$

$$\omega_g = angular\ velocity\ from\ the\ gyroscope$$

$$\theta_a = angle\ from\ the\ data\ of\ accelerometer$$

The following equation calculates filter coefficient:

$$\alpha = \frac{\tau}{\tau + dt} \tag{8}$$

Whereas,

$$\tau = Time\ constant\ of\ the\ filter$$

In this thesis, the complementary filter is implemented with the help of the PI (proportional integral) controller rather than using the time constants. The complementary filter with PI controller is shown in the figure 9:

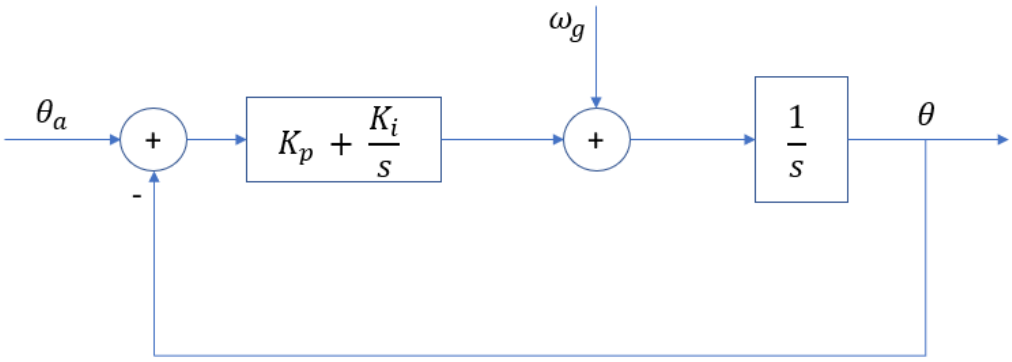

Figure 9: Complementary Filter with PI controller

The complementary filter in figure 9 is acting as the low pass filter for the angle calculated from accelerometer in order to have accurate steady state response. While acting as the high pass filter for the gyroscope in order to have accurate transient response. The reason behind using this type of the complementary filter is that it does required any resetting of the values in the real time motion. While the complementary filter implemented with time constant requires the resetting of the filter constant after the motion from one position to another.

Complementary filter is fast in estimating angle and does not show any lag during the calculation. Furthermore, complementary filter is not very computationally intensive [12].

2.3 Trajectory Planning

Control system for the manipulator needs to be developed in order to perform desired tasks. The type and number of sensor installed on the manipulator have significant impact on deciding, how a control system should be designed. Depending on the demand of situation, a control system can be either open loop or close loop system. In other words, in order to make the manipulator to follow the predetermined path we need a system which includes the controller and appropriate sensors. A typical control system for position control demands information from the sensors like current position. This information is compared to the desired position hence error is generated which is given to the controller. The controller then commands the movement of the manipulator in order to follow the path. The system is usually a closed loop control system i.e. a feedback is given to the controller. The error between current and desired position can be reduced by using such systems. Whereas open loop system does not contain the feedback, so it is not able to correct itself. For this reason open loop system is usually operated manually [17]. The overview of the closed-loop is shown in the figure below:

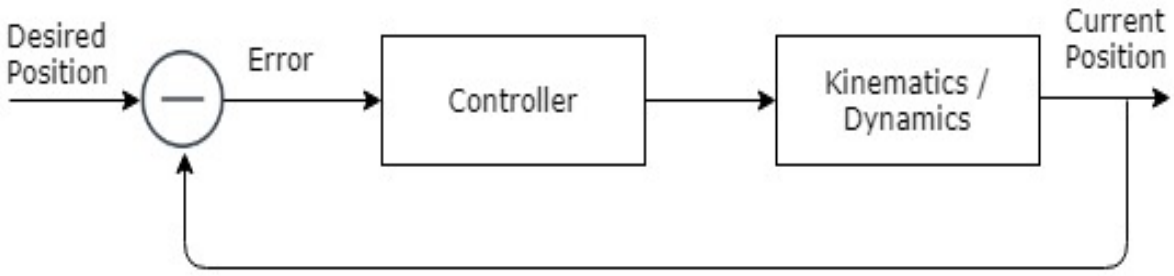

Figure 10: Closed-Loop control System [17]

Nowadays, Industrial robots are playing an important role in automating our industries. For this reason, industrial robots need to have high flexibility to perform different technological operations where robot movements can be compared to the human flexibility. In order to achieve such flexibility, the trajectory of the robot must be smooth and close to optimal. The robot should also be able to avoid the obstacles. Such performance demands effective trajectory planning. Trajectory planning decides the feasible motion from the initial position of the manipulator to the final position after considering kinematics and dynamic constraints [18]. With trajectory planning, interim intermediate positions are generated between current and final position so that manipulator could follow the desired path. Trajectory planning can be done in the joint space or in the Cartesian space [18]. Trajectory planning in the joint space is comparably easy because the joint variables are defined with respect to the time. This simplifies calculations required to compute the values for joint variables. This method is straightforward as equation of inverse kinematics are not needed [17]. On the contrary, trajectory planning in cartesian space is not as straight forward. The path of the end-effector is constructed with respect to time along with its position and orientation. However, this method of planning is more intuitive in nature [19].

The idea of trajectory planning further widens after deciding the operational space i.e. whether the space is joint space or cartesian space. In the next step, we decide the motion constraints i.e. point to point trajectory planning or the path motion (multi point trajectory planning). Point to point trajectory planning is done for the material handling tasks, because point to point is enough for assigning pick-up and release locations of an abject. This means that the manipulator has to follow the path from the initial joint configuration to the final joint configuration in the allotted time. While the path motion is used mainly for machining task in which manipulator has to follow the multiple points according to the order of the desired path. In conclusion, the purpose of the trajectory planning is to calculate the desired variable for the joint or end-effector with respect to the time for a desired motion [20]. An overview of the trajectory planning is given in the figure below:

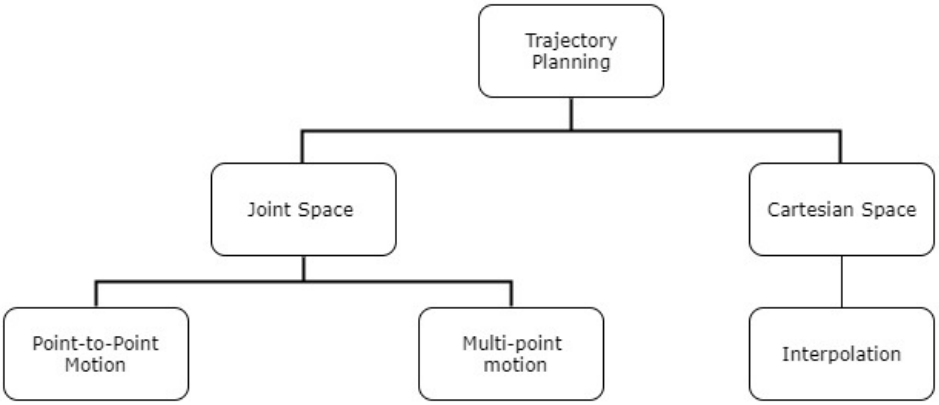

Figure 11: Overview of Trajectory Planning [20]

Polynomials are used to implement the trajectory planning. Order of the polynomial determines how many variables can be computed during trajectory planning, with single order polynomial only positions can be controlled. With increasing the order of the polynomial, velocity and acceleration of the manipulator can also be controlled. Trajectory planning ensures the smooth trajectory from one position to another i.e. no abrupt changes in the position consistency. Moreover, the trajectory must be free from the kinematics singularities [21]. On these conditions order of the polynomial is decided. Higher order of polynomials has high accuracy and better results. However, the increase in accuracy comes at the cost of computational power and time. Therefore, either you can achieve more accuracy or computational ease that best suits the targeted task.

In this thesis, point to point trajectory planning is being used. To implement point to point trajectory planning, first order polynomial is used. The reason behind the selection of this is the simple nature of the case. There is a single requirement for the movement of the hydraulic boom of the GIM machine is to control the position, during the motion from one position to the another with respect to time. Higher order of polynomial computation is not being used because it is out of the scope of this thesis.

3. METHODOLOGY

3.1 System Configuration

In the earth moving project, the Generic Intelligent Machine (GIM) is equipped with boom and bucket which is used to dig and dump the pile at the user-defined positions. Multiple tasks have been carried out to complete the process form scooping to dumping. First of all, laser scanner on the GIM machine produces the ground model for the user. After this user analyses the ground model and defines the digging and dumping area, this process is known as high level planning. Once the areas are defined, this model is uploaded to the XPC target computer along with the other models, which includes the multiple subsystem blocks like dead reckoning, high level communication block, work hydraulics, navigation block and CAN UDP blocks. These subsystem plays their own role for the completion of the task. Detail overview of these blocks is beyond the scope of this thesis. After uploading the models, GIM machine works autonomously. Once the GIM machine reaches to its required position, work hydraulic blocks starts working, which gather the data of IMUs from the UDP blocks in order to determine the current position of the boom and the buckets through the principles of forward kinematics. After this work hydraulic block determines the errors between current position and pre-defined scooping position. This error is transmitted to the controller, which generates the commands for moving the boom and bucket to reach the desired position. These all subsystem works in real time and the processing of these subsystem is recursive and continuous during the whole process of scooping and dumping.

During the implementation process few issues arises that are needed to be solved for smooth operation. One of the issues, is the unnecessary oscillation of the boom and bucket while moving from the scooping to the dumping position and vice versa. Second problem is related to the positioning of boom in steady state. As the boom and the bucket are interlinked, mispositioning of boom can affect the position of the bucket. Therefore, often the bucket does not position parallel to the ground for scooping. Either it is pitched upward and is unable to penetrate in to the pile and GIM machine starts moving upward the pile or if it is pitched downward than it starts scrapping the ground, which ends the scooping operation due to sheer resistance.

This research has been carried out to solve these problems. So, the blocks under the scope of this thesis are the work hydraulic block and the CAN UDP block. As these blocks are used to gather the data from the IMUs for determining the current positions and for calculating error in order to reach desired position. The overview and working of these blocks is as shown in the flowchart given below:

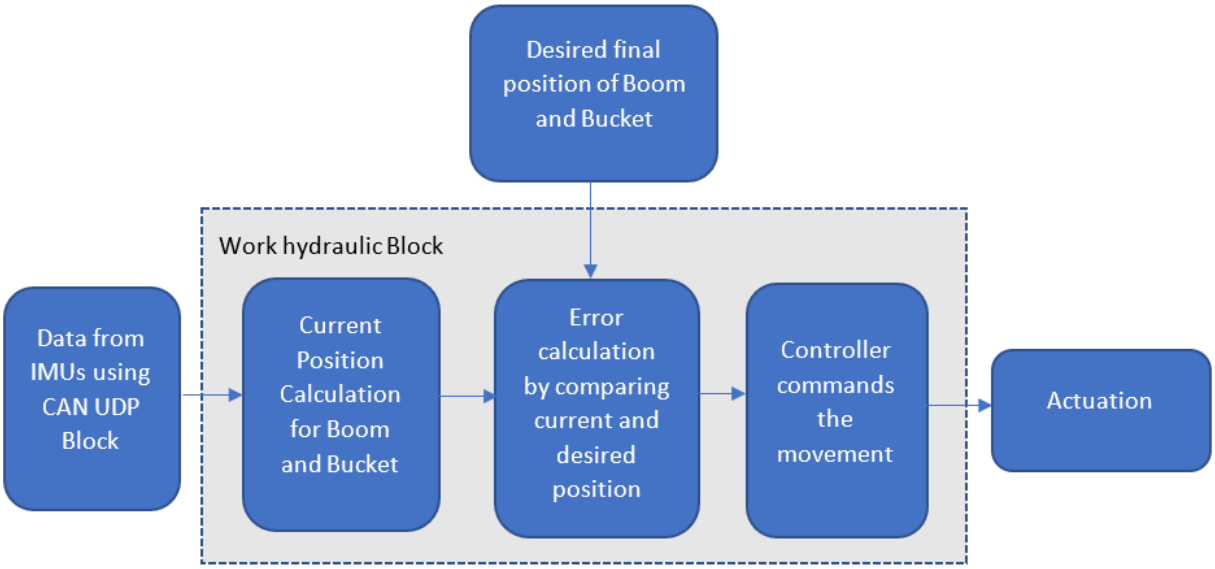

Figure 12: Overview of Boom Bucket Positioning

In the above diagram, the subsystem of work hydraulic block is illustrated that how data is processed in this block. Now the detailed overview of CAN UDP block will be illustrated in the figure 13:

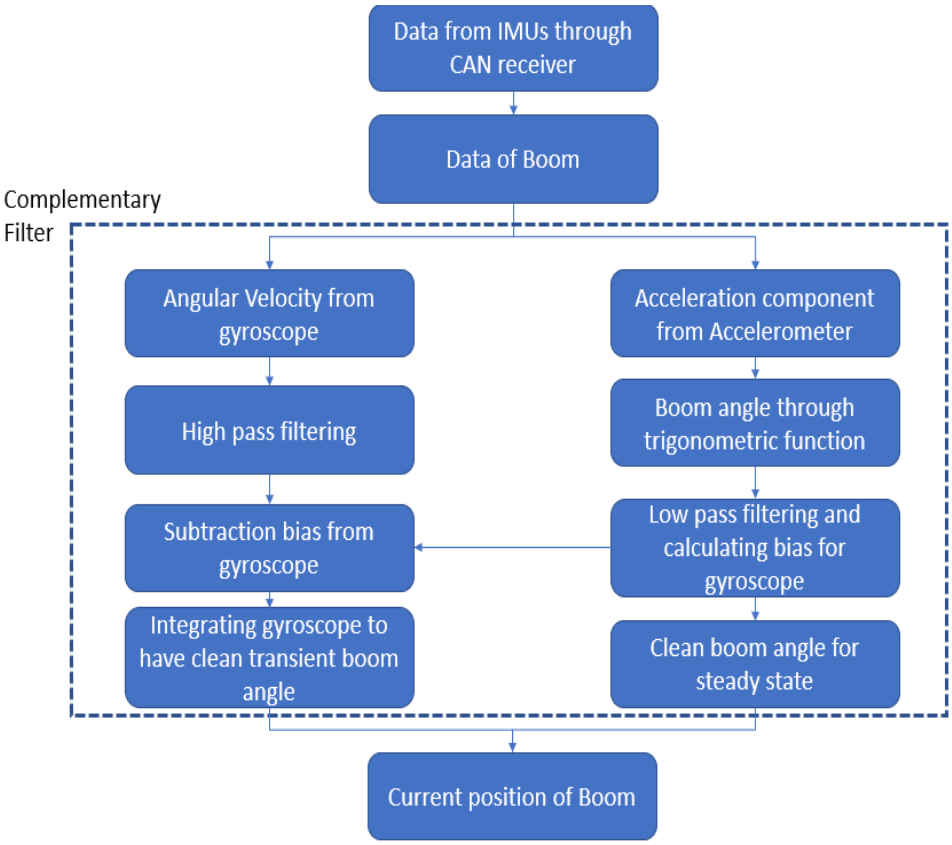

Figure 13: Current position measurement in CAN UDP block

Figure 13 illustrates the process of measurement for the current position of the boom. This same arrangement is also done for the measurement of the current position of the bucket in the CAN UDP block.

3.2 Limitations of Current System

Several problems have been reported in the autonomous earth moving project. This thesis will highlight some of the problems and devise appropriate solution for them. A core problem is the unnecessary oscillation of the boom and the bucket while moving from one position to another position such as scooping to dumping position. This issue arises because the actuation of boom and bucket is not synchronized. Although they are interlinked with each other, the movement of bucket is faster compared to the boom. This is due to the fact, that controller commands the actuation based on the error between the current and the desired position. The bucket minimizes its error quickly compared to the error correction in boom position, as it is still in the phase of error minimization. This delayed correction in the movement of the boom induces further error in the position of the bucket. As a result, unnecessary oscillation occurs in the movement of the boom and the bucket.

Another problem faced is the positioning of boom in the steady state, because the boom angle has oscillation which undermines its accuracy. This problem leads to the mis-positioning of the manipulator in steady state effecting the earth moving operations. In current system, complementary filter is used to determine the boom angle which provides the clean transients responses from gyroscope. However, the steady state response from accelerometer contain oscillations because the linear accelerations are not being removed from accelerometer data.

3.3 Approaches to solve limitations

In this thesis, we will discuss two different approaches to solve the above-mentioned limitations of the system. First approach tries to synchronize the moment of the boom and the bucket. In this approach, trajectory planning is introduced with which interim intermediate positions are created between current and the desired final position. Now errors are calculated between the current position and the intermediate position. Unlike the current system now the error is divided according to the user defined positions instead of sending the whole value of error between current and final position to the controllers. This approach will help to synchronize the motion of the boom and bucket with both taking the same number of steps to reduce the error at the same sample time.

In the second approach, measurement process of current position of boom is altered in order to achieve the desired results. In this approach, the data of accelerometer will be processed prior to the complementary filter. As the data of accelerometer contains the angular acceleration as well as the linear accelerations, these linear accelerations are

needed to be removed in order to have clean steady state response. For implementing this technique, boom of the GIM machine is considered as a one link system and linear accelerations are being calculated for this system. Afterwards, these linear accelerations are removed from the data of accelerometer.

3.4 Software for Implementation

3.4.1 Simulink

Matlab has a special graphical modelling environment known as Simulink. It is used for simulation and model-based design. Apart from this Simulink is also used for generation of C/C++ codes along with continuous testing and verification of embedded systems. Simulink gives much of the things under the same roof as graphical editor, block libraries that can be modified and simulating dynamic systems. Furthermore, it is integrated with Matlab which helps to integrate the Matlab code in the model. [21]

Model-based design is the fast and easiest way of making the dynamic system. In model-based design, system model is developed after considering and analyzing the requirements and the goals for the system. The model can be refined anytime throughout the development process. After development, simulation of the model is created which illustrates whether the model is fine or not. Simulink is the suitable environment for developing model-based designs. In Simulink, models can be created using the block from the pre-defined libraries. These blocks can be connected with each other having a hierarchical relation between them. This way of modelling organizes the system as well as defining them at the same time according to their working. Simulink also allows to build the subsystem as per requirement of the signal or the dynamic system. [22]

3.4.2 Simulator

In AUT laboratory, R&D Hardware in the loop (HIL) simulator is developed for the research of autonomous mobile machines. In this simulator hydraulic system and mechanic designs are created same as of the real machine. Control system developed in this simulator is also close to the real machine as it uses the feedback control and the filter parameters. Furthermore, sensor fusion for navigation is also introduced which is capable of doing path planning and obstacle avoidance along with the development and testing enabling autonomous driving and manipulation.

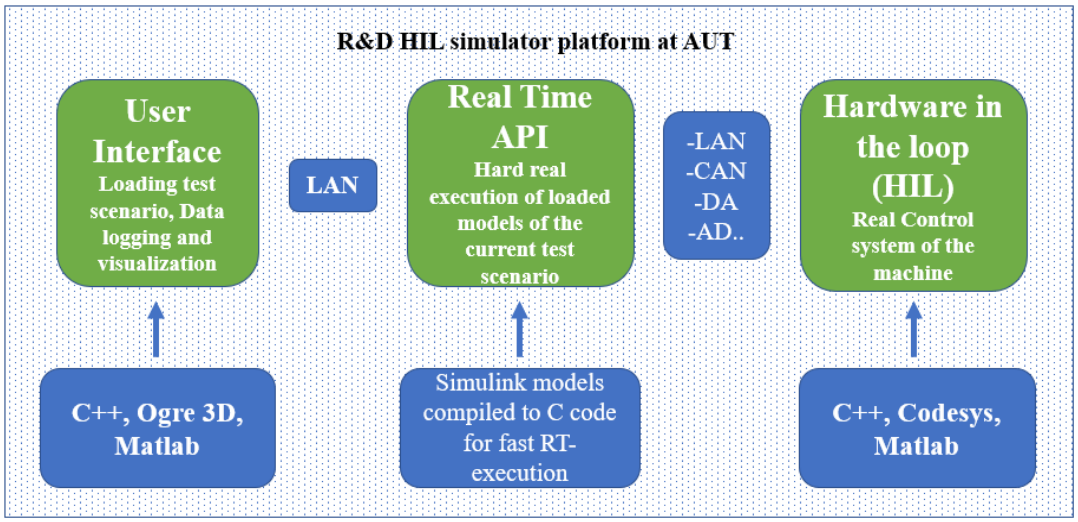

Figure 14: Overview of Simulator

3.4.3 Real machine data

This data is obtained from the sensors of the GIM machine using XPC target. This data contains the values from all the IMUs that are placed on the base, boom and the bucket. Furthermore, it also includes the data from the encoder placed on the telescopic joint of the boom. Data set which is under the scope of this thesis contains the values of the IMU which is placed on the boom. The required data set has three values one value from the gyroscope as it is one axis gyroscope (g_x), while two values from the accelerometer. Two values from the accelerometer (x_i and z_i) are the components of the gravity along the axis of the boom (x_b) and perpendicular to the axis of the boom (z_b). These values are shown in figure 15. These values are further processed to find the position and orientation of the boom.

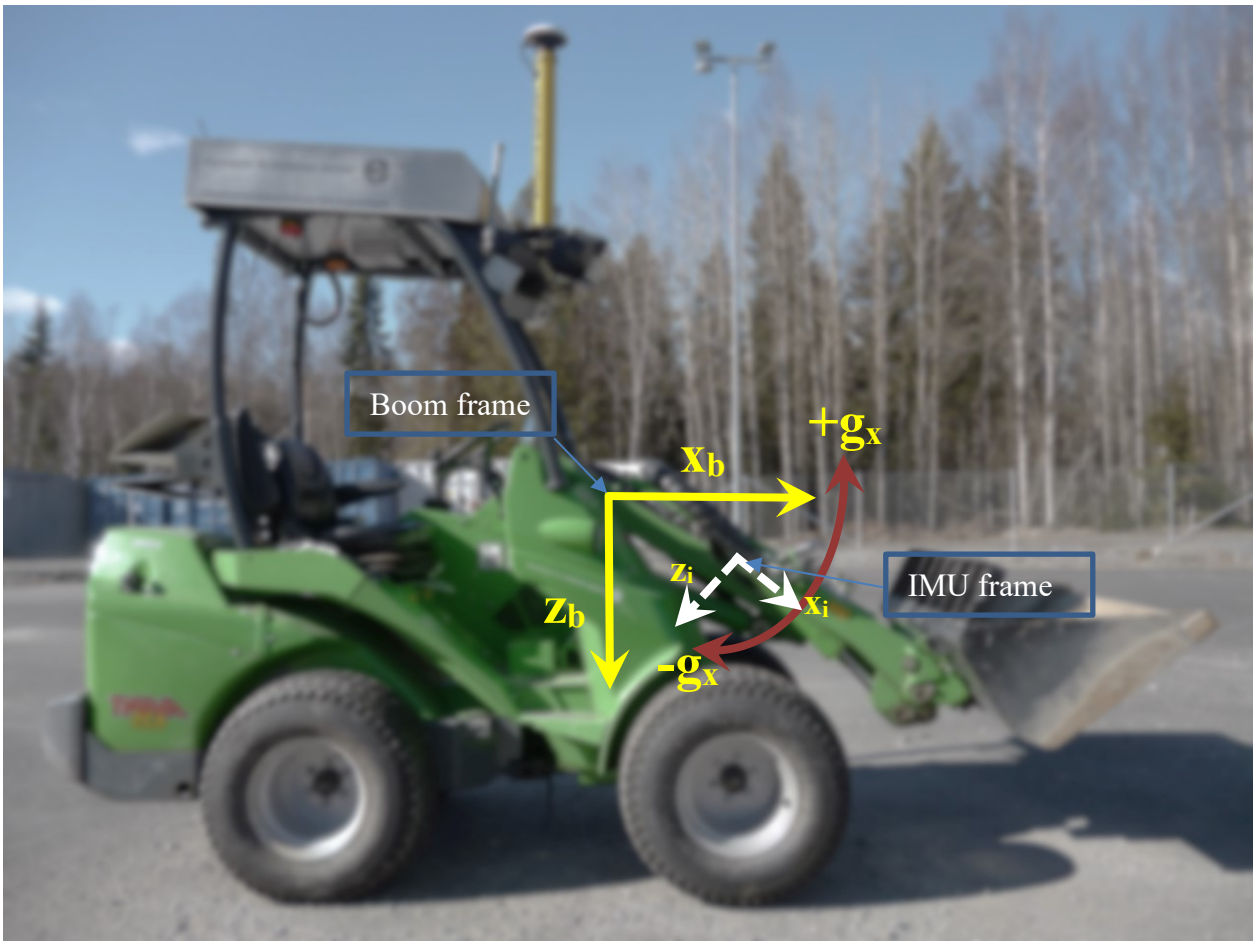

Figure 15: Illustration of Real machine data

4. TRAJECTORY PLANNING

As presented in the previous chapter, the unnecessary oscillation occurring in the GIM machine while scooping and dumping the pile causes a decrease in the efficiency of the task, as it is performed repeatedly. The main reason for the oscillation is the non-synchronal motion of boom and bucket. To solve the problem of synchronization, trajectory planning is introduced so that the interim intermediate positions are added between the current and desired position. In this way, the bucket, and the boom both reach the desired position at the same time in a synchronized way. Dividing the error in interim intermediate positions also create a smooth path for the boom and the bucket to move from the current to the desired position.

The position of scoop, haul and dump are defined by using a point on the GIM machine denoted as 'FF'. Position of FF is at the end of the boom where is the joint of the bucket. Thus, FF has the position of boom in x-direction and z-direction as well as the orientation of bucket as shown in the figure 16. The FF point can be represented in the following manner:

$$FF = \begin{bmatrix} x \\ z \\ \theta \end{bmatrix}$$

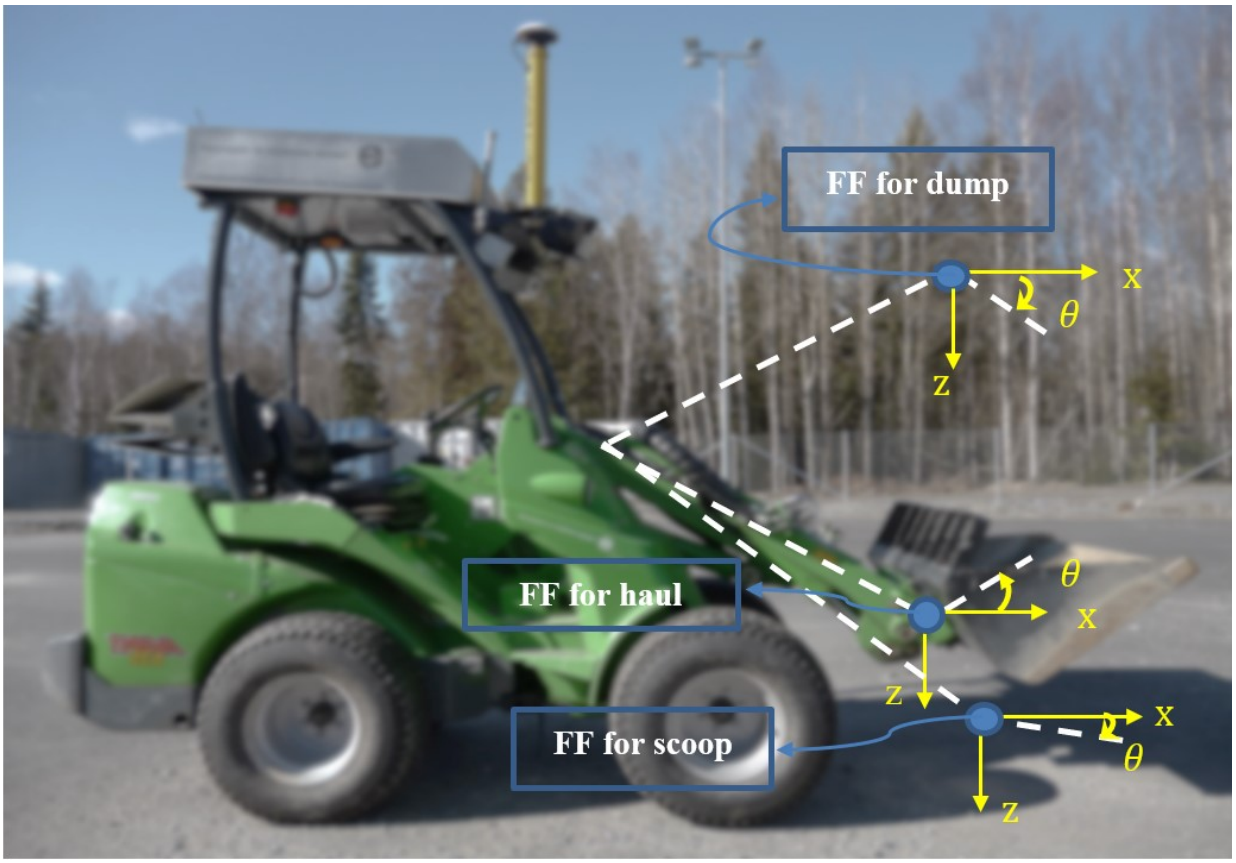

Figure 16: FF for scoop, haul and dump position

4.1 Implementation of Trajectory Planning

To solve the problem of unnecessary oscillations, trajectory planning is introduced for the motion from the current position to the desired position. For implementing trajectory planning, single order polynomial is used as the system is working in two dimensions, x-direction and z-direction. With trajectory planning, movement of FF is controlled from the current position to the final position through point-to-point trajectory planning. The single order polynomial is used to implement the trajectory planning, which is as follows:

$$FF = (FF_f - FF_i)tau + FF_i \tag{9}$$

Whereas

$$FF_f = desired\ position\ of\ FF\ point\ as\ shown\ in\ figure\ 16$$

$$FF_i = Intial\ position\ of\ FF\ point$$

$$FF = Current\ position\ of\ Boom\ in\ x\ and\ z\ direction\ \&\ orientation\ of\ bucket$$

While

$$tau = \frac{1}{number\ of\ intermediate\ position\ defined} \tag{10}$$

'tau' ranges from 0 to 1. Tau increments on the basis of the required interim intermediate positions defined by the user. It means that if user defines 10 intermediate positions then it will increment by 0.1 but in the case of 20 intermediate position, it will increment by 0.05. Whereas if there are 5 intermediate position then it will increment by 0.2.

The working principle of trajectory planning is to follow a certain path to the desired position from the current position. With the equation of trajectory planning, path between initial and final position is divided according to the value of 'tau'. In this way, the actuation of boom and bucket is being done by the controller by using the divided error between the initial position and the next interim intermediate position. Controller actuates the boom and bucket until the error between the current and the interim position reaches equal to or less than 0.06 m, the value of 'tau' will be increments and next intermediate position is calculated. Afterwards, the new value of error is given to the controller on the basis of new intermediate position. This process of incrementing 'tau' is recursive until the value of 'tau' reaches 1. The reason behind using 0.06 m as threshold distance because there is error of 10 cm during the motion of the manipulator of the GIM machine. It means that there can be error of 10 cm between the FF point and the desired position during the motion.

The implementation of trajectory planning is shown with the help of trajectory planning in figure 17:

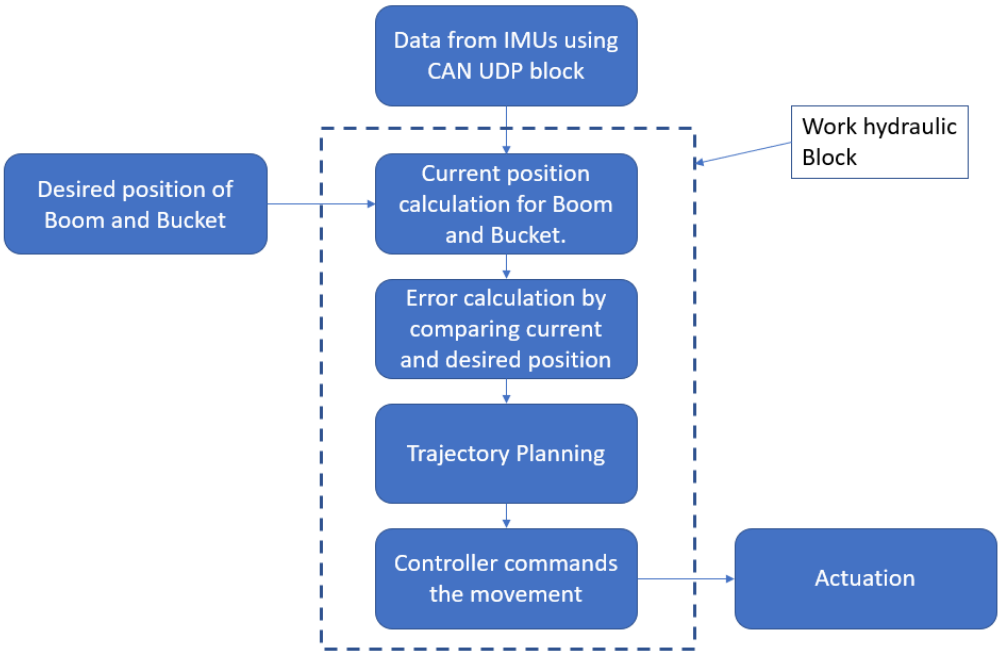

Figure 17: Current positioning of Boom and Bucket with Trajectory Planning

4.2 Procedure for testing Trajectory planning

Trajectory planning (TP) has been introduced in the model with three different set of final positions that are scoop, haul and dump. The trajectory planning is implemented with different number of intermediate positions, which are 5, then 10 and finally with 20 positions between current and the final position. After making the amendments in the system, these models are ready to be checked in the simulator. Once the model is uploaded in the simulator then actuating commands are given for checking the results of the system.

Test cycle created for the model is the movement of FF from scoop to haul then to dump and finally again to scoop position. Commands are given to the simulator are same and in the same pattern. First of all, command is given for scoop position then for haul position after that for dump position and finally again for the scoop position. Values of these positions are fixed for all the model which are as follows:

Table 1: Position & Orientation of FF at different states

	x	z	θ
Scoop	0.6	0.23	-5
Haul	0.8	-0.4	40
Dump	0.6	-0.85	-45
Scoop	0.6	0.23	-5

Values in the table 1 are the positions for FF as shown in the figure 16. These are values which determines the current and the final position.

To analyze the trajectory planning, movement of the FF will be shown in the graphs that how the values of FF changes in x-direction and z-direction as well as the orientation of the bucket in order to achieve desired position. Individual graphs are produced for the movement of FF on x-direction, y-direction and the orientation of bucket for all the models that are original model without trajectory planning, the models of trajectory planning having 5,10 and 20 intermediate positions individually. Every graph represents the result of the original model without any trajectory planning, and also the results of trajectory planning with 5, 10 and 20 steps.

4.3 Graphical Results

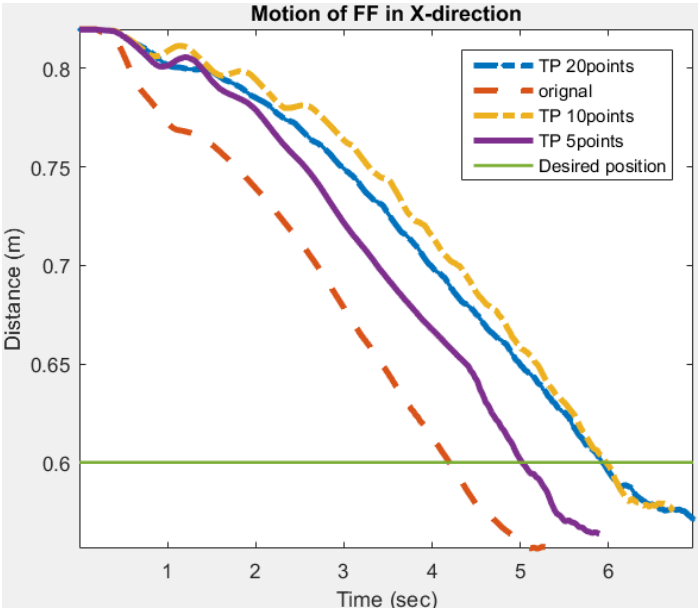

a

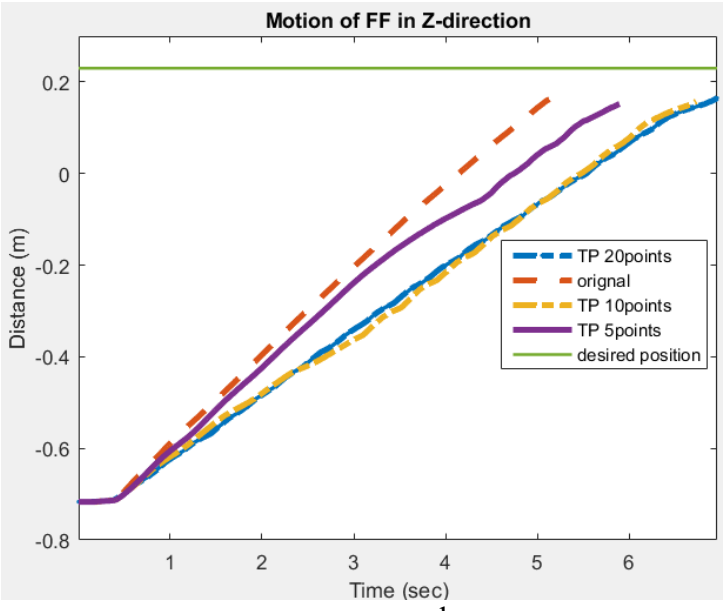

b

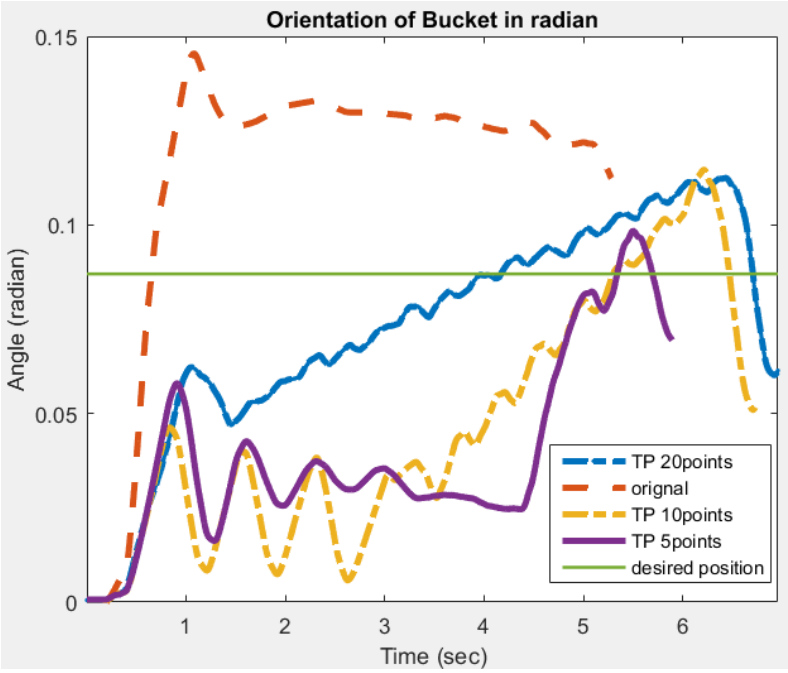

c

Figure 18: Motion from localized position to scoop position

Figure 18 shows the position and the orientation of FF from the localized position (as set in the simulator) to the scoop position. Figure 18a and b show the trajectory of FF in the x-direction and z-direction. While figure 18c shows the change in orientation of the bucket during the motion. The movement of boom shows no overshoot in the original model and the models implemented with trajectory planning, as the error is reducing gradually. While the movement of bucket shows the overshoot in the original model, showing that the boom and bucket are non-synchronized in reducing error in the original model. The reason behind these oscillations is that the bucket reduced its error before the boom, so the bucket has to adjust itself again when the boom reaches its desired position. While the figure 18c illustrates that the model with trajectory planning having 20 steps changes the orientation gradually while moving from localized to desired orientation so the movement of boom and bucket is synchronized having no oscillations. But the model with trajectory planning shows slight oscillations upon reaching the desired position. It is also clear from the figure 18 that the models with trajectory planning have the slow response as compared to original model as the trajectory planning causes smooth motion of the bucket and the boom. Moreover, there is always a difference in the desired position and orientation, and the actual final position and orientation achieved by the bucket and the boom. Further, comparison will be done in table 2.

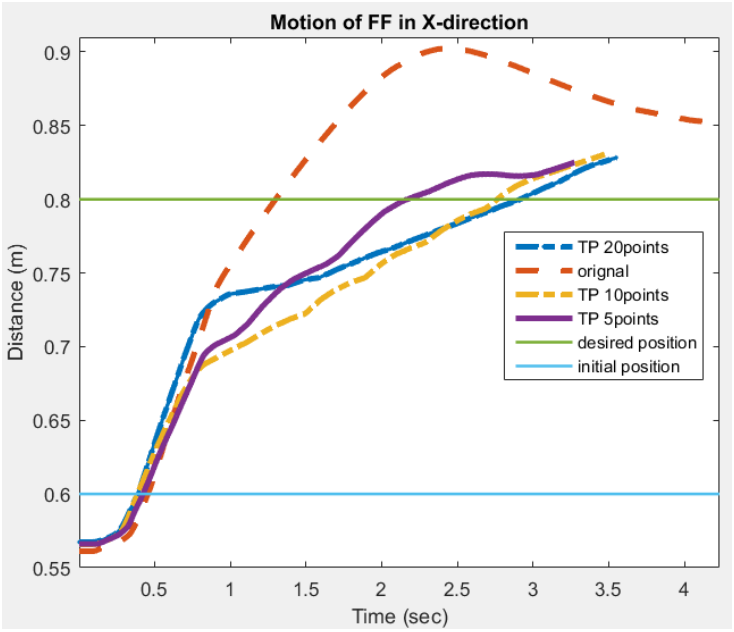

a

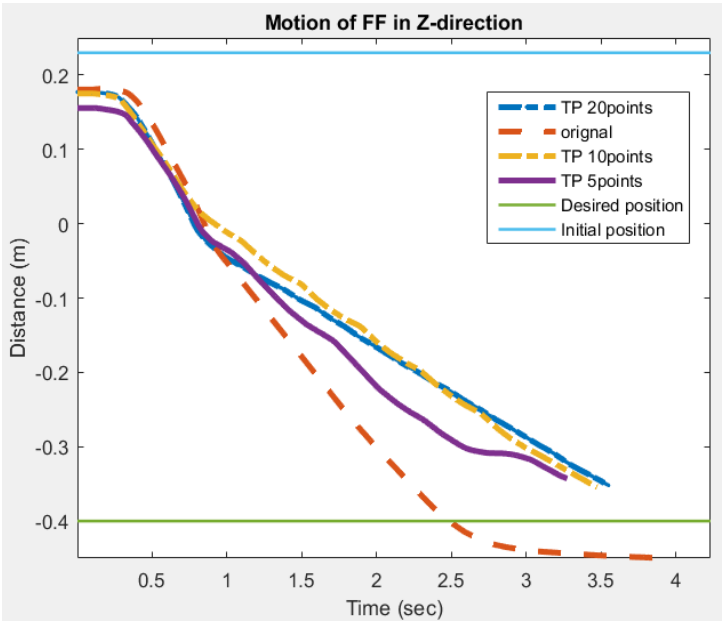

b

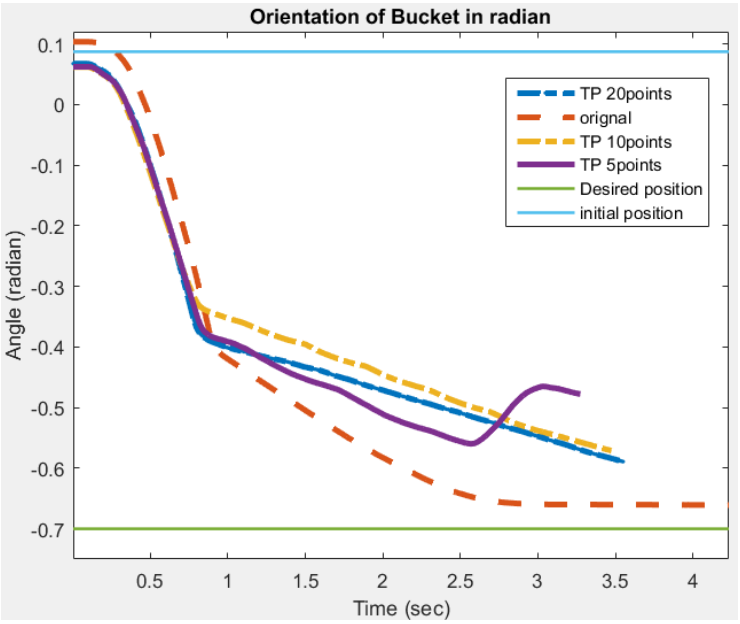

c

Figure 19: Motion from scoop position to the haul position

Figure 19 shows the position and orientation of FF from the scoop position to the haul position. In figure 19, initial position is the scoop position of FF reached in the figure 18. There is an offset between the starting point of the models and the initial position because of the accumulated error from the previous motion. Figure 19 a and b shows the moment of the boom in x-direction and in z-direction respectively. It can be seen from the figure 19a and b that the error in the boom is minimizing before the error in the bucket in the original model. Therefore, there are overshoots in the movement of the boom. However, the models with trajectory planning gradually minimizes the error and have no

overshoots, this proves that the motion of boom and bucket are synchronized during the motion in the models implemented with trajectory planning. Further, comparison will be done in table 3.

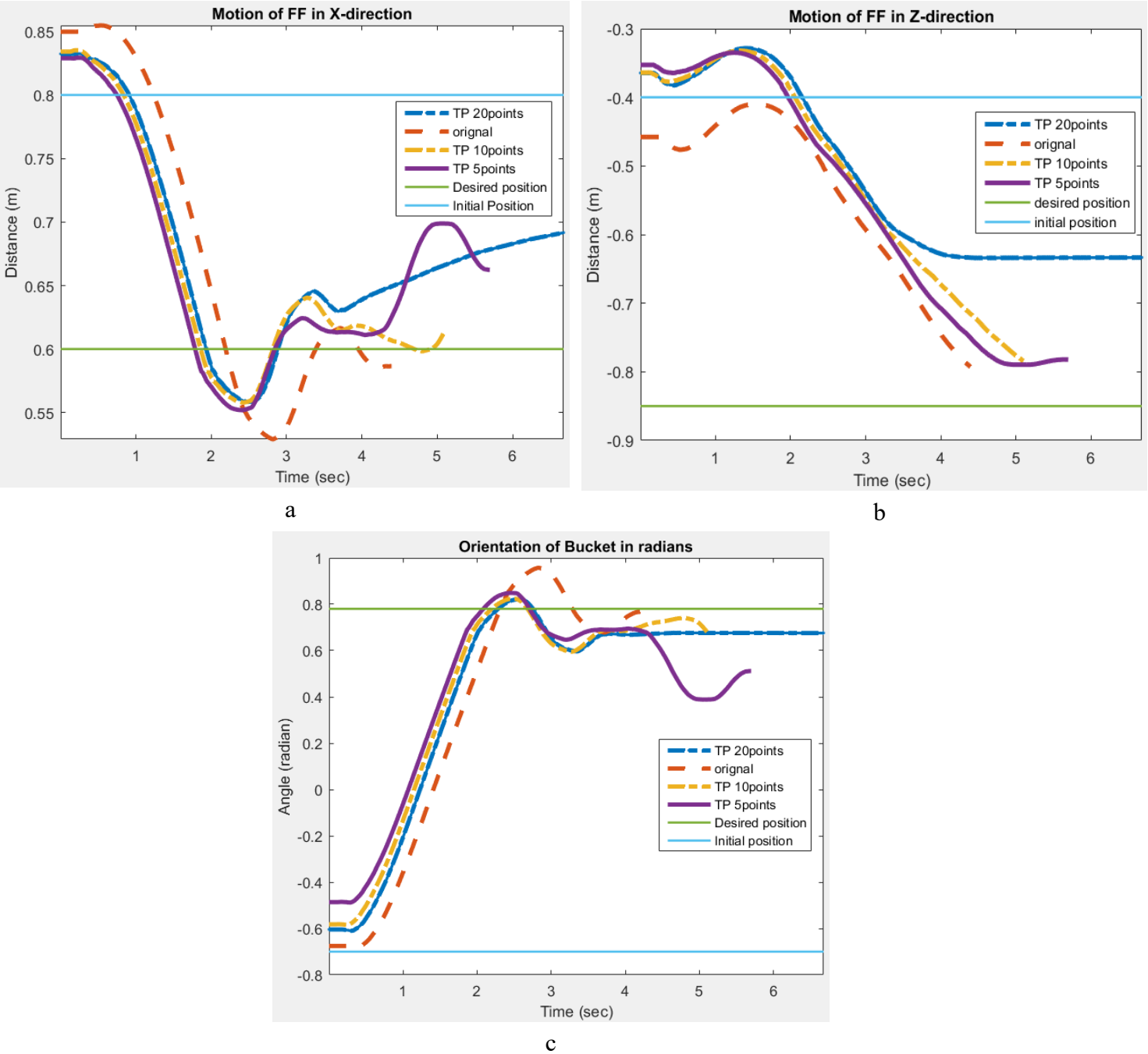

Figure 20: Motion from Haul to Dump position

Figure 20 shows the position and orientation of FF from the haul position to the dump position. In figure 20, initial position is the haul position of FF reached in the figure 19. This figure also contains the offset between the starting point of the models and the initial position as of figure 19, because of the accumulated error from the previous motion. In

figure 20, all the models contain the overshoots because bucket is minimizing the error faster than the boom, because boom and bucket are not synchronized. It is also evident from the figures that the models implemented with trajectory planning have less overshoots than the original model, showing models with trajectory planning synchronizing the motion of the boom and the bucket. Further, comparison will be done in table 4.

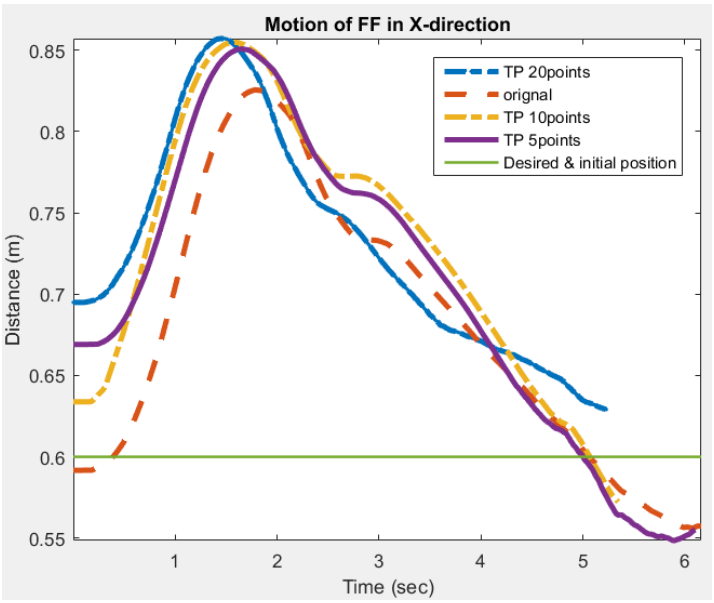

a

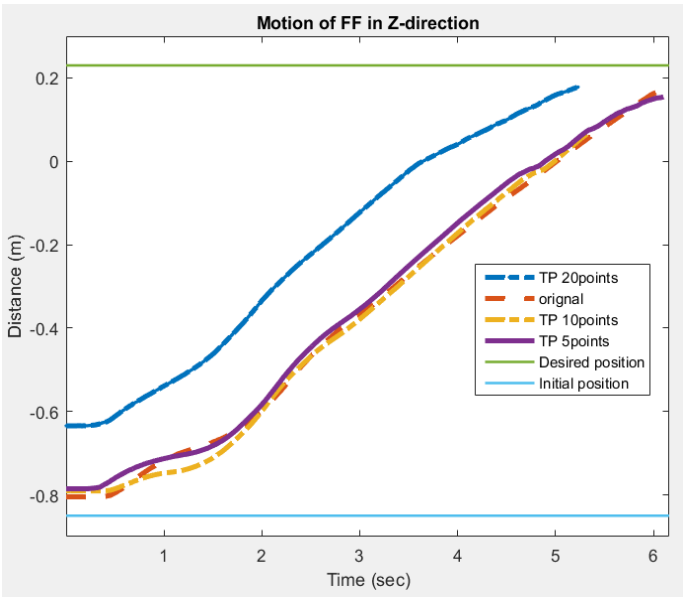

b

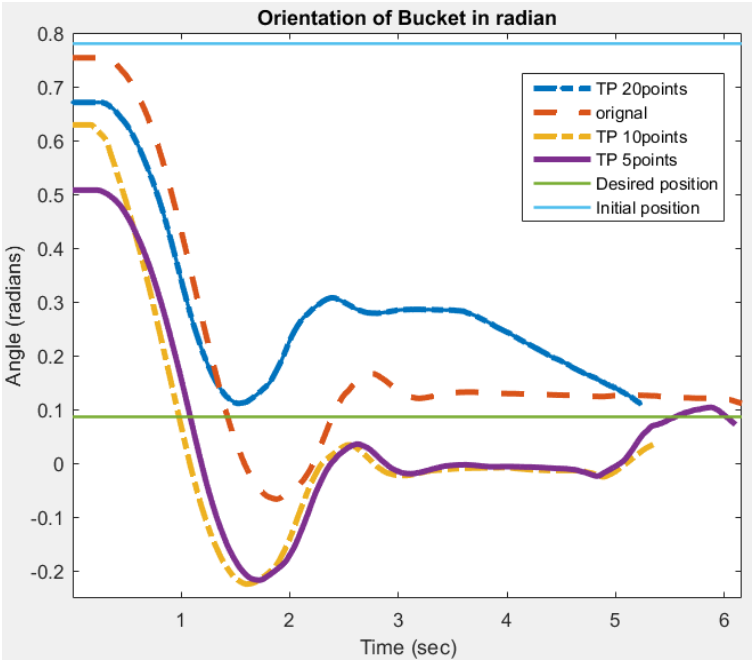

c

Figure 21: Motion from Dump to Scoop position

Figure 21 demonstrates the position of FF from the dump position to the scoop position. These figures also portraying the offset between the initial position and starting point of

the model because of accumulated error. In figure 21, there are overshoot in all the model while moving from the dump to the scoop position, because of the non-synchronal motion of the boom and the bucket. However, the model with trajectory planning having 20 steps has less oscillations compared to the original model because of the synchronous motion between the boom and the bucket. Further, comparison will be done in table 5.

4.4 Results Comparison

Table 2: Comparison from localized position to Scoop position

	Original Model	**Model with TP having 5 steps**	**Model with TP having 10 steps**	**Model with TP having 20 steps**
Overshoot	Yes	Yes	No, but contains the harmonic motion to desired position	No
Response Time	Fast	slow	slowest	slow
Steady State positioning	Reaching the desired position within the acceptable error	Reaching the desired position within acceptable error	Reaching the desired position within acceptable error.	Desired position acquired but show oscillation at the end

Table 3: Comparison from scoop to haul position

	Original Model	**Model with TP having 5 steps**	**Model with TP having 10 steps**	**Model with TP having 20 steps**
Overshoot	Yes	No	No	No
Response Time	Fast	slow	slowest	Slower than 5 steps but faster than 10 steps
Steady State positioning	Reaching to desired position within acceptable error range	Reaching to desired position within acceptable error range	Desired positions acquired with small error.	Desired position acquired with small error

Table 4 : Comparison from Haul to dump position

	Original Model	Model with TP having 5 steps	Model with TP having 10 steps	Model with TP having 20 steps
Overshoot	Yes	Yes	Yes, but less than the original model	Yes
Response Time	slowest	Fastest	slow	slow
Steady State positioning	Reaching Dump position within acceptable error	Not reaching to Dump position.	Dump position acquired with slight error	Model stopped in the middle during the motion to desired position

Table 5: comparison from dump to scoop again

	Original Model	Model with TP having 5 steps	Model with TP having 10 steps	Model with TP having 20 steps
Overshoot	Yes	Yes, large overshoot	Yes, but overshoot is less than the original model	Yes, but overshoot is less than the original model
Response Time	Slowest	Slowest	Slow	Fastest
Steady State positioning	Reaching to desired position within acceptable error.	Reaching to desired position within acceptable error.	Desired position acquired with small error	Desired position acquired with small error

5. IMU FILTERING

In this chapter, an approach to improve the angle estimation of the boom is explained. Current system calculates the boom angle using the complementary filter. The complementary filter performs multiple tasks as it acts as the high pass filter for gyroscope while performing the low pass filtering for accelerometer, Moreover, it also calculates the bias for the gyroscope using accelerometer. Complementary filter produces the transient response of the system using the values from the gyroscope while the results for steady state response is calculated from the values of the accelerometer. Major issue with the current ongoing system is that the angle is not accurate in the steady state. The reason is that the accelerometer data contains the linear acceleration in addition to the angular acceleration, which results in inaccurate angle estimation for the steady state. The removal of linear acceleration is performed prior to the complementary filter.

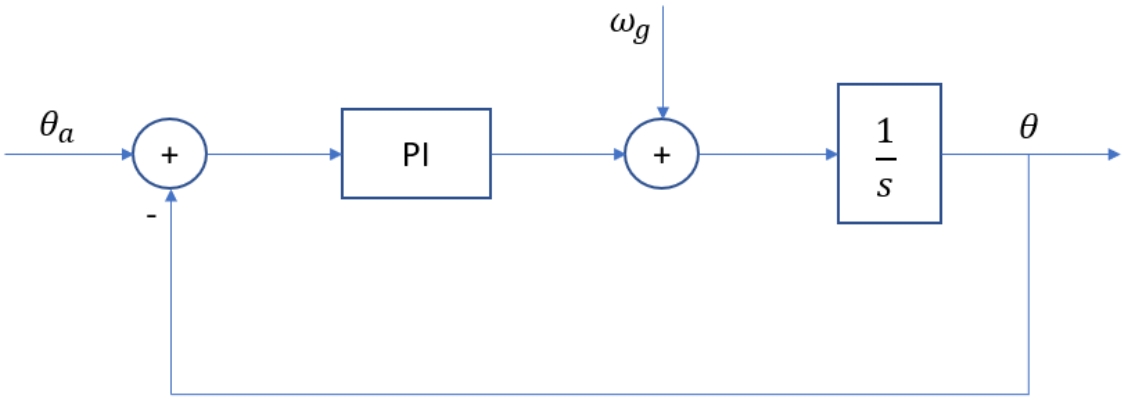

Figure 22: Complementary filter

In the above figure 22, θ_a is the angle calculated from the accelerometer while $\omega_g$is the angular velocity from gyroscope. The error for the PI (proportional integral) controller is calculated using the negative feedback of the boom angle θ and the angle θ_a calculated using accelerometers. The PI controller further calculates the bias for the gyroscope as shown in the figure 22. Furthermore, this PI controller also performs the low pass filtering for accelerometer and high-pass filtering for the gyroscope data. The corrected gyroscope data is then integrated to produce the boom angle θ.

5.1 Algorithm for calculating linear accelerations

In order to build the filter some assumptions are made such as the boom of the GIM machine is considered as a one link system as show in the figure below:

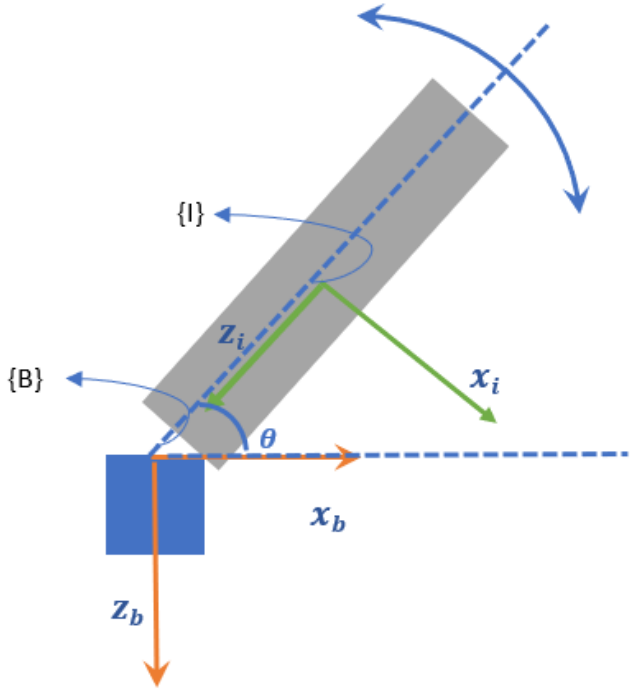

Figure 23: One link system with IMU

Figure 23 shows the one link system with the link having IMU frame {I}(OXZ) in the middle of the link and the boom frame {B}(OXZ) at the joint. Linear accelerations of this system are calculated at the IMU frame with respect to the boom frame. These linear accelerations are removed from accelerometer data to make the accelerometer angle accurate. While θ is the boom angle.

These are the following equation in order to calculate the linear acceleration of the boom.

$$V_x = 0 \tag{11}$$

$$V_y = 0 \tag{12}$$

$$V_z = L\dot{\theta} \tag{13}$$

$$^{b}V = {}^{b}R_i \begin{bmatrix} 0 \\ 0 \\ L\dot{\theta} \end{bmatrix} \tag{14}$$

Where V_x is the linear velocity in x-direction of the boom frame {B}, V_y is the linear velocity in y-direction of the boom frame and V_z is the linear velocity in z-direction of boom frame {B}. Whereas L is the distance between the IMU frame {I} and the boom frame {B}. ^{b}V is the linear velocity of the link in boom frame {B}. whereas $^{b}R_i$ is the rotation matrix for transforming the IMU frame {I}to the boom frame {B}. $^{b}R_i$ rotation

matrix contains the rotation about y-axis of the boom frame {B} according to the angle of the boom.

$$^{b}R_i = R_y(\theta)$$

$$^{b}R_i = \begin{bmatrix} \cos\theta & 0 & \sin\theta \\ 0 & 1 & 0 \\ -\sin\theta & 0 & \cos\theta \end{bmatrix} \tag{15}$$

After adding equation (15) in equation (14), we get the following equation

$$^{b}V = \begin{bmatrix} L\dot{\theta}\sin\theta \\ 0 \\ L\dot{\theta}\cos\theta \end{bmatrix} \tag{16}$$

Considering movement of the boom in x-direction and z-direction, we neglect y-direction so ^{b}V is as follows:

$$^{b}V = \begin{bmatrix} L\dot{\theta}\sin\theta \\ -L\dot{\theta}\cos\theta \end{bmatrix} \tag{17}$$

Derivating equation (17), we get

$$\begin{bmatrix} a_{lx} \\ a_{lz} \end{bmatrix} = \begin{bmatrix} L\ddot{\theta}\sin\theta + L\dot{\theta}^2\cos\theta \\ L\ddot{\theta}\cos\theta - L\dot{\theta}^2\sin\theta \end{bmatrix} \tag{18}$$

Where

$$a_{lx} = L\ddot{\theta}\sin\theta + L\dot{\theta}^2\cos\theta \tag{19}$$

$$a_{lz} = L\ddot{\theta}\cos\theta - L\dot{\theta}^2\sin\theta \tag{20}$$

After getting the final equation of linear accelerations. These linear accelerations are required to be removed from the respective data of the accelerometer that is a_x and a_z.

5.2 Block Diagram for removal of linear acceleration

The implementation of the improved filter is shown in the figure below as the block diagram:

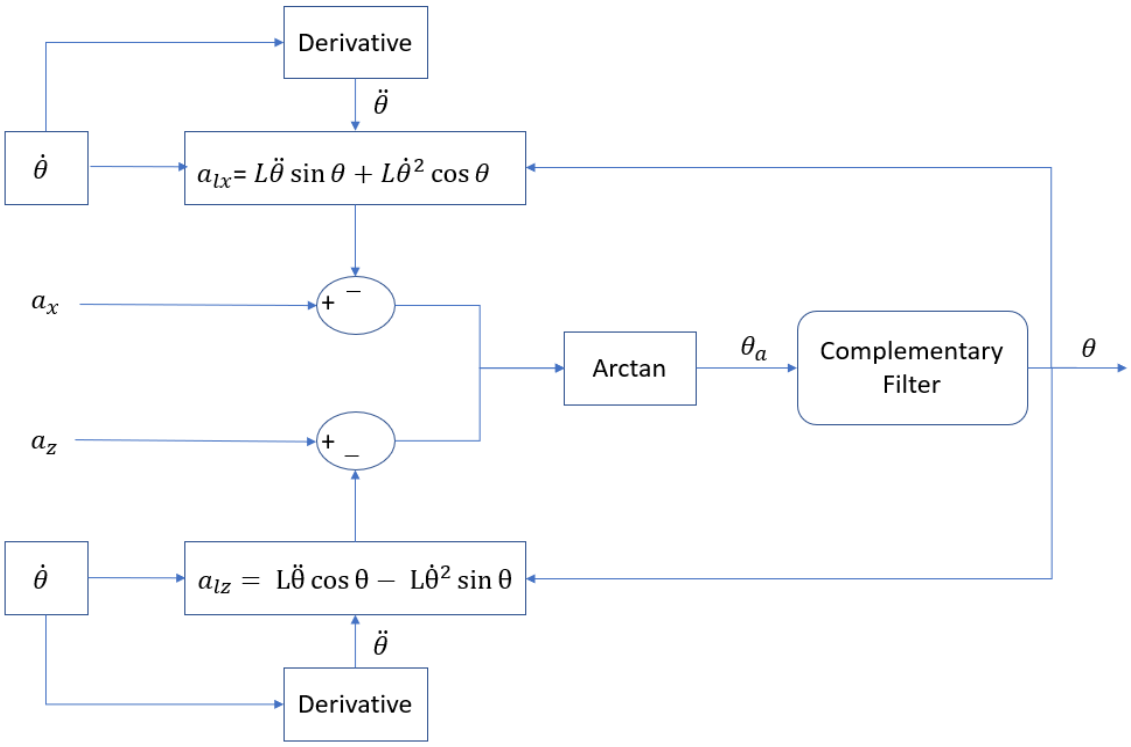

Figure 24: Block Diagram for removing linear acceleration

Figure 24 shows the three inputs for determining the linear acceleration in the respective direction. One of the input is angular velocity i.e. $\dot{\theta}$, which comes from the gyroscope, while second input is the derivative of angular velocity which is denoted as $\ddot{\theta}$. Finally, third input is the boom angle denoted by θ. After calculating the linear accelerations, these accelerations are removed from the data of accelerometer in their respective directions. After removing linear acceleration, angle is being calculated which is denoted as θ_a. This angle is one of the input for the complementary filter for calculating boom angle denoted as θ.

5.3 Data Set from GIM machine

Data of accelerometer is collected for the movement of hydraulic manipulator of GIM machine, which contains two revolute joints and one prismatic joint. Two revolute joints are for boom and bucket. First the boom is moved upwards to maximum limit of the boom joints, then it is being moved downwards till the minimum limit of boom joint. After this boom is moved approximately to the middle of the joint, in order to analyze the effect of motion of other joints on the boom. In order to check the effect of other joints, afterwards, prismatic joint is extended and retracted to its maximum and minimum position. After this bucket joint is moved to its maximum and minimum limit. These movement of other joints is being carried out while boom is stationary.

5.4 Results of IMU filtering

Plot of Boom angle for original model and proposed model for entire motion

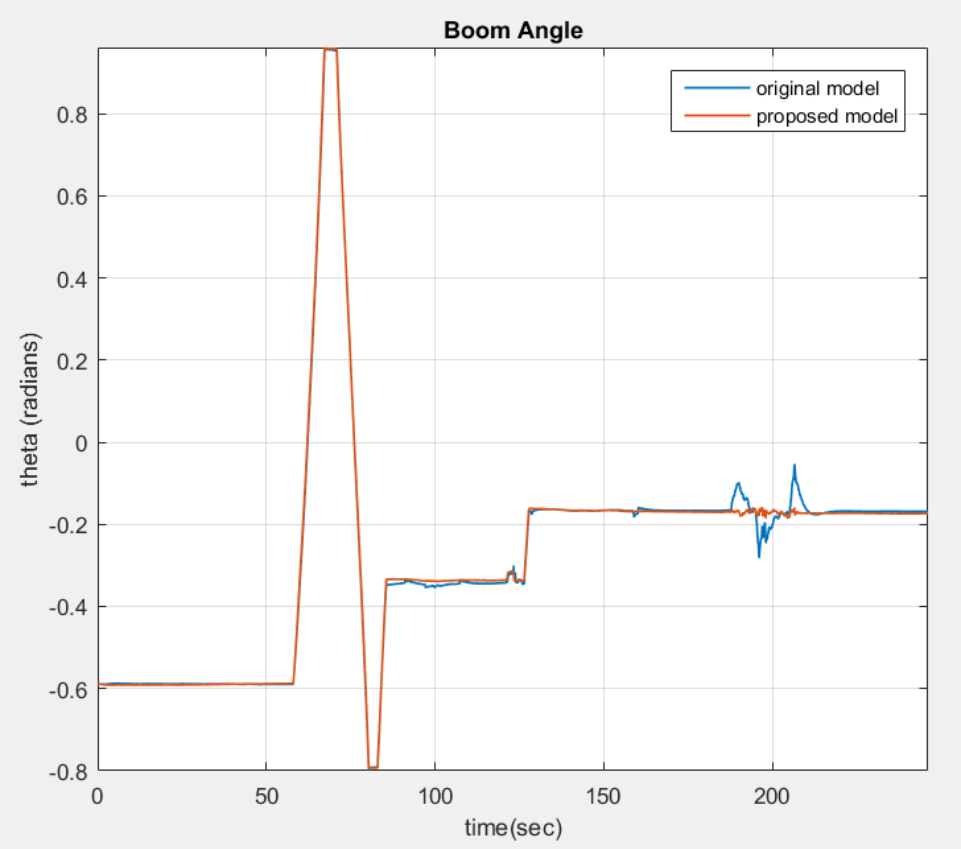

Figure 25: Boom angle for original model and proposed model for entire motion

Figure 26 illustrates the angle of boom during its movement. At approx. time stamp 55 to 70 boom is moving upwards to its maximum position. Then approx. during time stamp 70 to 75 seconds boom is at the maximum position and this is also the steady state of the boom for its maximum position. After this boom is moved to the minimum position downwards and it reaches the minimum position at approx. time stamp 85 seconds. Then the steady state exists till approx. time stamp 90 seconds. Later on, boom is moved upwards to the localized position at approx. time stamp 130 seconds. At this stage, boom will remain stationary and the other joints are moved. This test is being done in order to check the effect of the motion of other joints on the steady state of the boom.

Figure 26 describes that the transient response of the boom is almost same for the original model and the proposed model during its motion upwards to the maximum position and to the minimum position downwards. However, results have been improved during steady states and it can be seen that oscillation of the boom angle is reduced during steady state.

These are results are discussed in detail by presenting the region of interests at different locations of figure 26.

Comparison of transient response of the boom angle between original model and proposed model:

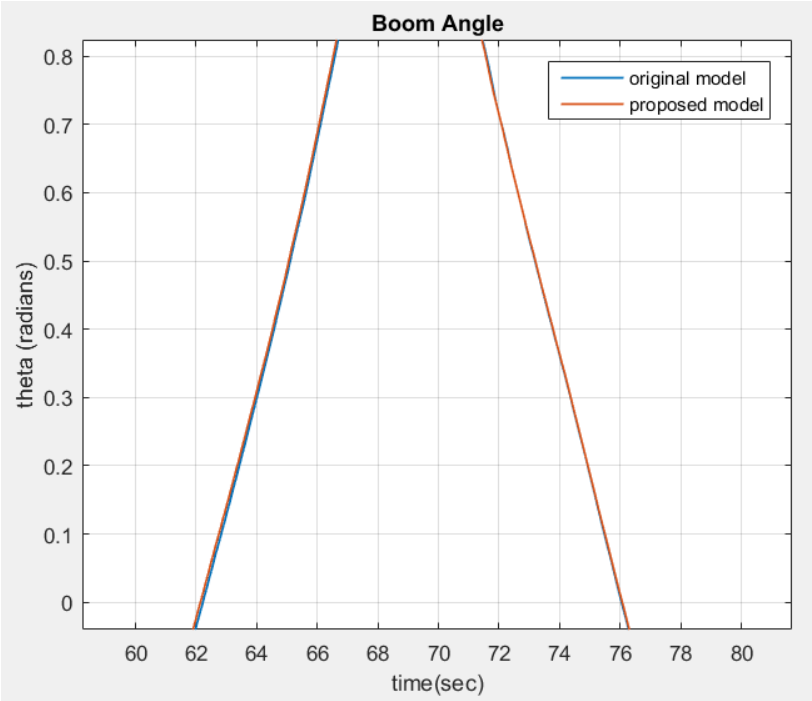

Figure 26: Transient response of the boom movement

In figure 27, the area of interest is shown between approx. time stamp 62 to 76 for describing the transient response of boom during the motion to the maximum position and then to the minimum position. Figure 27 demonstrates that the smooth change of boom angle for the proposed model and for the original model during the entire motion of boom.

Comparison of steady state response of the boom angle between original model and proposed model:

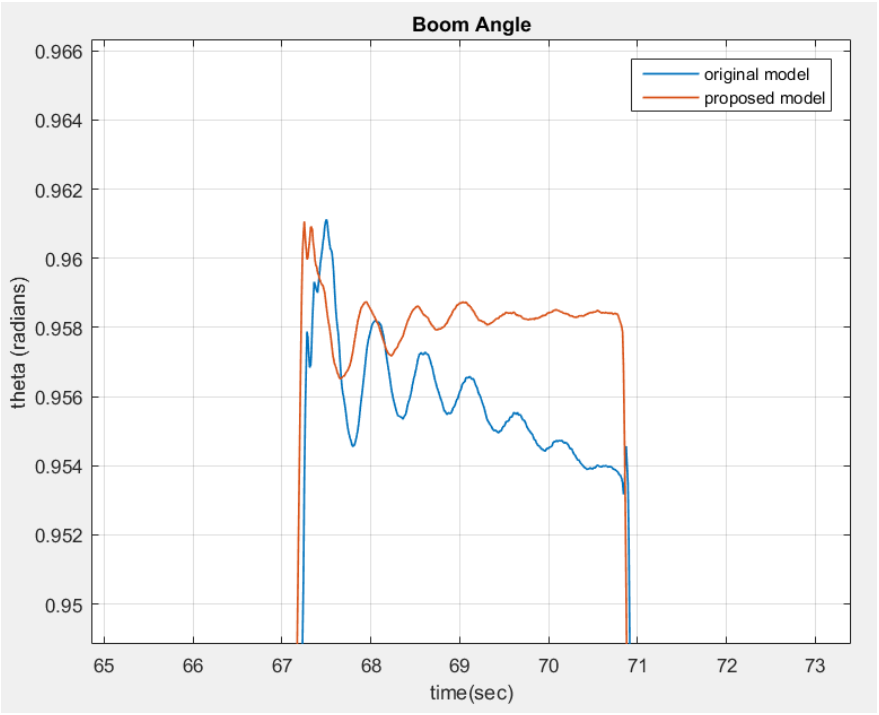

Figure 27: steady state response of boom when it reaches to maximum position

In figure 28, the area of interest is approx. for time stamp 67 seconds to 71 seconds for demonstrating the steady state response of the boom after reaching maximum position. Figure 28 illustrates that the response of the proposed model is improved as it has the less oscillation compared to the original model.

Steady state boom angle between original model and proposed for the motion to the localized position

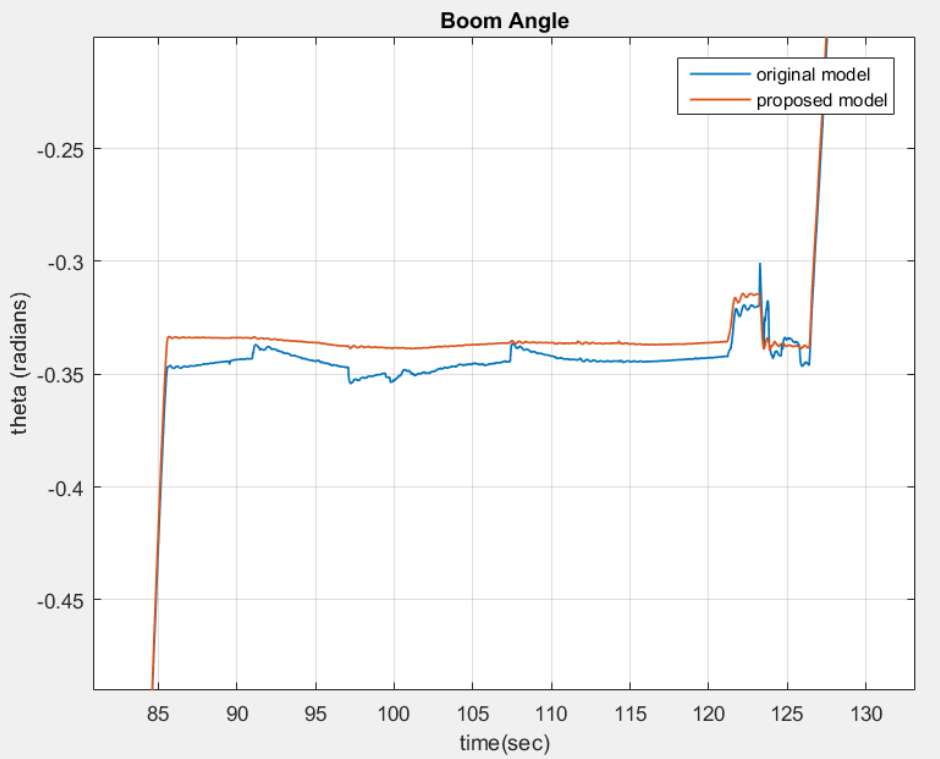

Figure 28: Steady state response during movement to localized position

Figure 29 illustrates the steady state response of the boom at the localized position after the motion from the minimum position. This plot clearly shows that the proposed model has smooth results as compared to the original model.

Effect on the boom angle of the motion of other joints

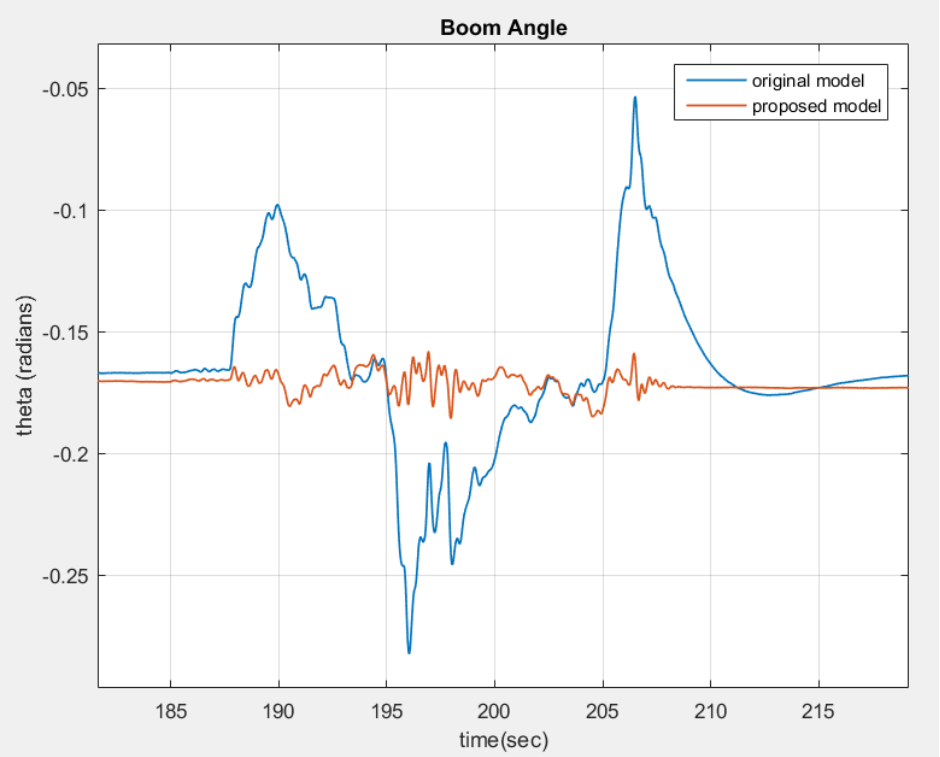

Figure 29: Effect on boom angle of the motion of bucket and prismatic joint

Figure 30 demonstrate how the movement of revolute joint of bucket and prismatic joint effects the steady state response of the boom angle. It can be seen in the figure 30 that movement of revolute joint of bucket and prismatic joint produces vibrations and jerks in the boom, which generates linear accelerations in the boom. That's why, after removal of linear acceleration results are improved as shown in the figure 30. Thus, improving the steady state response of the boom.

Plots for linear accelerations

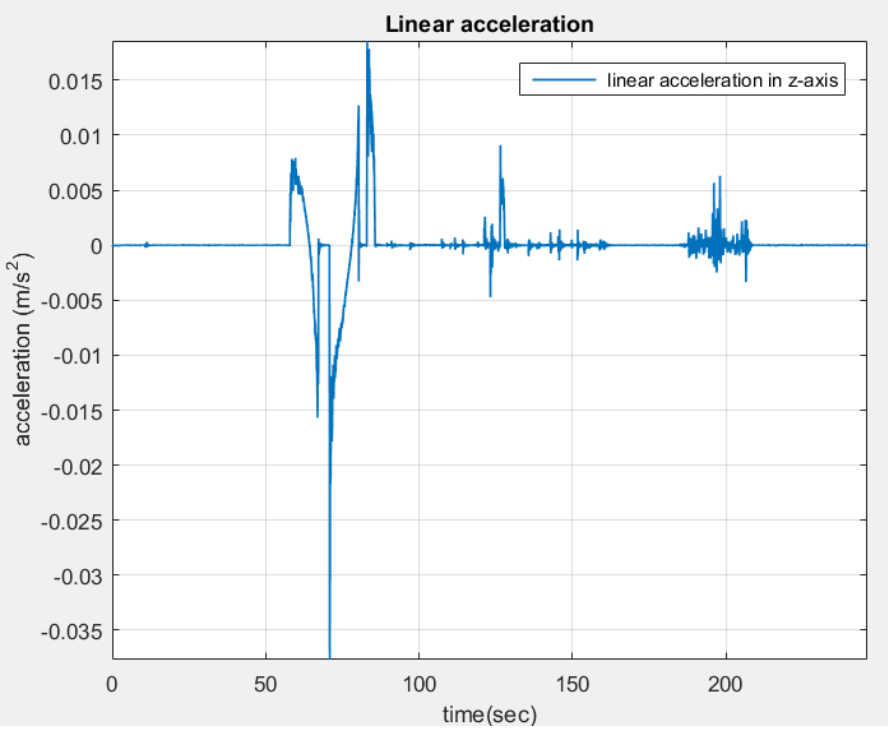

Figure 30:Linear acceleration in z-direction

Figure 30 demonstrates the linear acceleration in the z-direction. It shows that there are significant linear accelerations whenever the movement of boom starts its motion as shown at approx. time stamp 60 seconds or when the boom reaches the desired position as shown at approx. time stamp 70 seconds. This proposition is further supported at approx. time stamp 75 seconds when boom started moving to its minimum position downwards and approx. at time stamp 85 seconds when the boom reaches its minimum limit. Figure 30 also illustrates the substantial linear acceleration during approx. time stamp 180 seconds to 220 seconds when the boom is still, and revolute joint of bucket and prismatic joint are moving, as their movement produces the vibration and jerks in the boom.

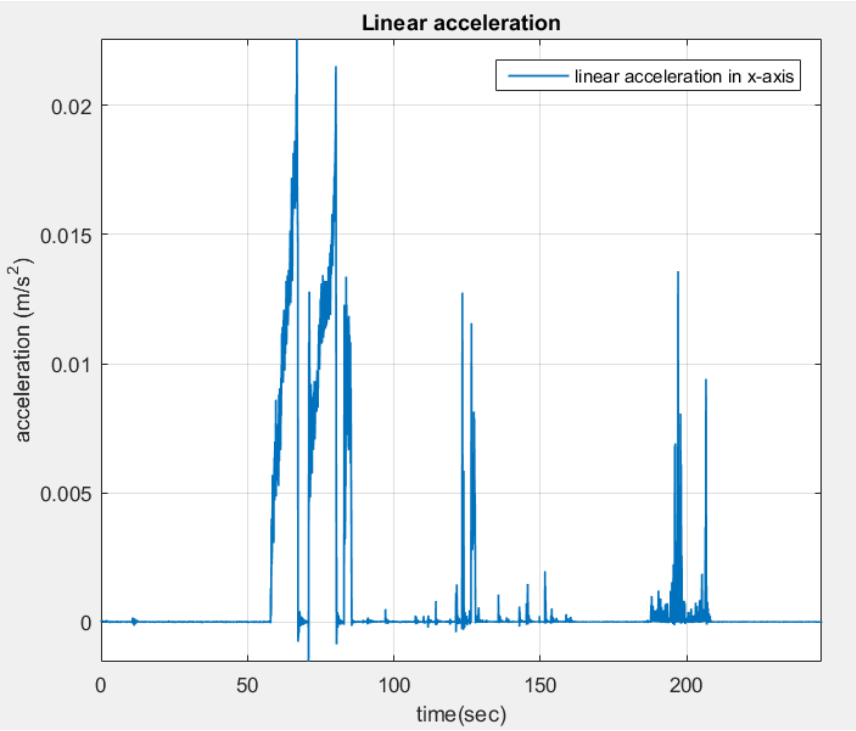

Figure 31:Linear acceleration in x-axis

Figure 31 illustrates the linear acceleration in x-axis. Figure 31 has the linear acceleration approx. at the same time stamp as that of figure 30 but their values are different from figure 30. Figure 31 also shows that there are linear accelerations whenever boom starts its movement or when it reaches to its desired position as shown at approx. time stamp 60 seconds and 70 seconds. Figure 31 also illustrates that there are significant linear accelerations during approx. time stamp 180 seconds to 220 seconds. During this time boom is stationary while the revolute joint of bucket and prismatic joint is in motion.

5.5 Quantitative Analysis

In order to analyze the results quantitively, root mean square (RMS) error of boom angle calculated from the original model are compared to the RMS error of boom angle calculated from the proposed model. For better comparison, the RMS errors are compared during the transient state, then the steady state, and also when the boom is the stationary while other joints are moving. These values are illustrated in table 6:

Table 6: Quantitative analysis of Boom angle

	RMS error of Original Model	RMS error of proposed model
Boom angle during transient state	0.0050	0.0043
Boom angle during steady state	0.0055	0.0044
Movement of other joints while boom joint is stationary	0.0372	0.0062

Table 6 verifies that the proposed model has better results than the original model. As the RMS values of the proposed model is less than the values of original model. This analysis also demonstrates that the proposed model reduces the overshoots in the boom angle. It can be seen from the table that the RMS error is almost same during the transient state as the removal of linear acceleration has the least effect during that state. While the result for the steady state is improved as the RMS value of proposed model is less than the original model, because the linear acceleration produced from the jerk by boom is removed from the values of the accelerometer, when it reaches its maximum limit. Finally, table 6 verifies that results are improved a lot for the boom angle, when the boom is stationary while other joints are in motion. The reason behind this improvement is the removal of linear acceleration produced due to the jerks and vibration from the movement of other joints.

6. CONCLUSION

This chapter concludes the research being done over the course of this thesis. The chapter present the goals that have been achieved by the proposed approaches. Furthermore, it provides an overview of the challenges that remain and what could be done in future to solve these challenges.

One of the problem in the autonomous earth moving project is the unnecessary oscillation of the boom and bucket from the one state to another. The aim of this thesis work is to remove those oscillations. The proposed approach suggests introducing the trajectory planning for smooth transition from the one state to another. Through trajectory planning, interim intermediate positions are introduced between the initial and the final position. This approach forces the manipulator to follow the path as defined by the user. Moreover, it helps to divide the error according to the user defined positions since the error is calculated between the current and the interim position instead a single error value between the current and the desired position. In addition, this division of error helps to synchronize the motion of boom and the bucket leading to the smooth movement of the boom and bucket between different states. From the obtained results, it can be observed that the trajectory planning has significantly mitigated the unnecessary oscillations for some of the movements especially the trajectory which involves the movement from the localized position to the scoop position and from scoop to the haul position. However, this approach does not have the effective results for the movement from the haul to the dump position and from dump to the scoop position. It has also been observed from the results, that by introducing the trajectory planning the response time of the boom and the bucket increases compared to the original model. Moreover, all three models (5, 10 and 20 steps) with trajectory planning did not reach the exact desired position in the steady state but came within an acceptable range of the error. However, in the motion from haul to dump, the model of the trajectory planning based on 20 steps does not reach the acceptable range of steady state error. Nonetheless, it can be concluded that the model with trajectory planning has improved some of the motions of the boom and the bucket. Further details of the approach and results have been discussed in chapter 4.

The second issue reported in the autonomous earth moving project is the inaccurate boom angle in the steady state, which leads to the misalignment of the bucket while scooping i.e. the cutting blade is not parallel to the ground. To tackle this problem, improvement in the IMU filtering has been proposed. The major issue in the current approach is that the linear accelerations are not being removed from the accelerometer, as a result, the complementary filter is unable to produce the accurate steady state boom angle. For improving the IMU filtering, it is proposed to calculate the linear accelerations of the system and remove them from the values of the accelerometer prior to the use of the

complementary filter. The technique for calculating the linear acceleration and the obtained results have been shown in the chapter 5. The results confirm that the proposed solution can improve the boom angle calculated from the accelerometer in the steady state. However, the results from chapter 5 illustrates that the transient response of the original model and of the proposed model have the similar results, i.e. the smooth response for the movement from the localized position to the maximum position and from the maximum position to the minimum position. The results that are improved with the proposed solution are the steady state responses, when the boom reaches the maximum limit or minimum limit. It can be seen from the figures 27 and 28, that with the proposed solution boom reaches its desired positions with less oscillations and jerks as there are lesser overshoots. Moreover, to corroborate the results, a comparative case is studied for the boom angle, when the boom is stationary, and only the bucket joint and prismatic joint are moving. The results illustrate that the accuracy of the boom angle is improved, because the linear accelerations in the data of accelerometer are removed. As a result, less overshoots are observed in the boom angle.

REFERENCES

1. GIM - Finnish Centre of Excellence in Generic Intelligent Machines Research [Internet]. [cited 2018 Apr 22]. Available from: http://gim.aalto.fi/

2. Ghabcheloo R, Hyvonen M. Modeling and motion control of an articulated-frame-steering hydraulic mobile machine. In: 2009 17th Mediterranean Conference on Control and Automation. 2009. p. 92–7.

3. Siegwart R, Nourbakhsh IR, Scaramuzza D. Introduction to Autonomous Mobile Robots. MIT Press; 2011. 473 p.

4. Dudek G, Jenkin M. Inertial sensors, GPS, and odometry. In: Springer Handbook of Robotics. Springer; 2008. p. 477–490.

5. 4. Gyroscope Technology 1 - Knovel [Internet]. [cited 2018 Feb 6]. Available from: http://app.knovel.com/web/view/khtml/show.v/rcid:kpSINTE002/cid:kt003T2XA2/viewerType:khtml/?view=collapsed&zoom=1&page=1

6. Srinivasan S, Moreira R, Blumenthal D, Bowers JE. Design of integrated hybrid silicon waveguide optical gyroscope. Opt Express. 2014 Oct 20;22(21):24988.

7. Kelly A. Mobile robotics: mathematics, models and methods. New York, NY, USA: Cambridge University Press; 2013. 701 p.

8. Apostolyuk V. Coriolis Vibratory Gyroscopes [Internet]. Cham: Springer International Publishing; 2016 [cited 2018 Mar 1]. Available from: http://link.springer.com/10.1007/978-3-319-22198-4

9. 7. Accelerometers - Knovel [Internet]. [cited 2018 Feb 6]. Available from: https://app.knovel.com/web/view/khtml/show.v/rcid:kpIMEMSPP3/cid:kt008MUGB3/viewerType:khtml/root_slug:inertial-mems-principles/url_slug:accelerometers?&kpromoter=federation&b-toc-cid=kpIMEMSPP3&b-toc-url-slug=introduction&b-toc-title=Inertial%20MEMS%20-%20Principles%20and%20Practice&page=1&view=collapsed&zoom=1

10. Levinzon F. Piezoelectric Accelerometers with Integral Electronics [Internet]. Cham: Springer International Publishing; 2015 [cited 2018 Feb 6]. Available from: http://link.springer.com/10.1007/978-3-319-08078-9

11. Kovačević B, Banjac Z, Milosavljević M. Adaptive Filtering. In: Adaptive Digital Filters [Internet]. Berlin, Heidelberg: Springer Berlin Heidelberg; 2013 [cited 2018 Feb 7]. p. 31–73. Available from: http://link.springer.com/10.1007/978-3-642-33561-7_2

12. Gui P, Tang L, Mukhopadhyay S. MEMS based IMU for tilting measurement: Comparison of complementary and kalman filter based data fusion. In: Industrial

Electronics and Applications (ICIEA), 2015 IEEE 10th Conference on. IEEE; 2015. p. 2004–2009.

13. Colton S, Mentor FRC. The balance filter. Present Mass Inst Technol. 2007;

14. Valenti RG, Dryanovski I, Xiao J. Keeping a Good Attitude: A Quaternion-Based Orientation Filter for IMUs and MARGs. Sensors. 2015 Aug 6;15(8):19302–30.

15. Coopmans C, Jensen AM, Chen Y. Fractional-Order Complementary Filters for Small Unmanned Aerial System Navigation. J Intell Robot Syst. 2014 Jan;73(1–4):429–53.

16. Euston M, Coote P, Mahony R, Kim J, Hamel T. A complementary filter for attitude estimation of a fixed-wing UAV. In: 2008 IEEE/RSJ International Conference on Intelligent Robots and Systems. 2008. p. 340–5.

17. PÄKKILÄ S. MODELING AND SIMULATION OF A SIX DEGREES OF FREEDOM EXCAVATOR. 2017;

18. Liu H, Lai X, Wu W. Time-optimal and jerk-continuous trajectory planning for robot manipulators with kinematic constraints. Robot Comput-Integr Manuf. 2013 Apr 1;29(2):309–17.

19. Siciliano B, Sciavicco L, Villani L, Oriolo G. Robotics [Internet]. London: Springer London; 2009 [cited 2018 Feb 22]. (Grimble MJ, Johnson MA, editors. Advanced Textbooks in Control and Signal Processing). Available from: http://link.springer.com/10.1007/978-1-84628-642-1

20. Gasparetto A, Zanotto V. Optimal trajectory planning for industrial robots. Adv Eng Softw. 2010 Apr;41(4):548–56.

21. Simulink Documentation - MathWorks Nordic [Internet]. [cited 2018 Feb 13]. Available from: https://se.mathworks.com/help/simulink/index.html?s_tid=gn_loc_drop

22. Model-Based Design - MATLAB & Simulink - MathWorks Nordic [Internet]. [cited 2018 Feb 13]. Available from: https://se.mathworks.com/help/simulink/gs/model-based-design.html